Asian Journal of Chemical Sciences

12(2): 50-89, 2022; Article no.AJOCS.92374
ISSN: 2456-7795

Physico-chemical Characterization of Some Metal Complexes Formed by Substituted Thiourea

G. Swarnabala [a*], S. B. Khatavkar [b], G. S. Sadana [b] and Anahita Bharadwaj [c*]

[a] Swaram Biochem, Hyderabad, India.
[b] Research Laboratory, Chemistry Department, G. N. Khalsa College, Mumbai– 400019, India.
[c] Department of Agricultural & Biological Engineering, Penn State College, Pennsylvania, USA.

Authors' contributions

This work was carried out in collaboration among all authors. All authors read and approved the final manuscript.

Article Information

DOI: 10.9734/AJOCS/2022/v12i2218

Open Peer Review History:
This journal follows the Advanced Open Peer Review policy. Identity of the Reviewers, Editor(s) and additional Reviewers, peer review comments, different versions of the manuscript, comments of the editors, etc are available here: https://www.sdiarticle5.com/review-history/92374

Original Research Article

Received 03 August 2022
Accepted 06 October 2022
Published 21 October 2022

ABSTRACT

In view of unique physico-chemical observations affecting the geometry and various properties of the substituted thiourea complexes in literature along with several biological activities, N-(hydroxy)-N,N-diphenyl thiourea was taken up for study. Complexes with geometries of high spin octahedral for iron(II), cobalt(II); tetrahedral & square planar for nickel(II); and dimeric square planar for copper chloride, copper perchlorate, copper acetate and distorted octahedral for copper nitrate were synthesized and characterized based on magnetic moments, visible spectra, diffuse reflectance spectra, electron spin resonance, infrared spectral studies, and thermal analysis.

Interestingly, the nature of anion influenced the geometry, the complex from copper nitrate salt resulted in a distorted octahedral structure and complexes formed from copper chloride, copper perchlorate, copper acetate exhibited sub-normal magnetic moments, highly insoluble in the most common organic solvents and water. Based on these and spectral data, polymeric or square-planar dimeric geometry with sulfur bridging between copper atoms is proposed. It was confirmed by the application of Bleaney-Bower's equation for magnetic susceptibility, applicable to dimeric copper complexes.

The overall thermal behavior of the ligand and complexes were observed and the detailed calculations interestingly lead to confirmation of the above proposed geometrical structures.

**Corresponding author: E-mail: swarnabalaganti@gmail.com, anahita.b02@gmail.com;*

Keywords: Bleaney-bowers equation; polymeric complexes; thermal analysis; freeman and carroll equation; vosburgh and cooper method; job's continuous variation method.

1. INTRODUCTION

Numerous substituted thiourea compounds have been utilized as coordinating ligands for the formation of metal complexes [1-10 and 11 with references therein], considering the stereochemistry, site of the coordination, and the effect of the anions present in the metal salts used for their formation. These have coordination via sulfur, oxygen, intermolecular hydrogen bonds between sulfur and hydrogen on nitrogen, and possess antibacterial, antifungal, anti-tubercular, anti-thyroid, insecticidal properties and were studied for screening of several biological activities [12,13].

Complexes of N,N-substituted thioureas have been studied (11 with references therein) in detail such as for Ethylene thiourea, substituted thioureas, N,N-diethyl thiourea, S-acetyl thiourea and N,N phenyl thiourea which behave as bidentate chelating agents being bonded to metal through both nitrogen and sulfur atoms; complexes of 1-amidino-2-thiourea, N,N-ethylenebis(N-phenyl thiourea) have been investigated with the infrared spectral data in detail, the magnetic moments being normal at RT with electronic spectra showing low symmetry ligand fields; Ni(II) complexes assume Td, Oh or tetragonal geometry, with various degree of perturbations; Pd(II) and Pt(II) display fourfold coordination, but with strong tendency to form penta coordinated adducts; investigations of Co(II) complexes have pronounced tendency to form Td geometry, $[CoL_2X_2]$.

Polymeric complexes of Co(II) thiocyanate with thiourea and N-methtable
yl thiourea have been found (11 with references therein) Oh; with N,N-di(o-tolyl) thiourea pseudo-Td complexes, while Ni(II) complexes of these ligands are tetragonal; nitrogen coordination in thiourea or its derivatives is rare except in N-methyl thiourea complexes of Pd (II), Pt(II) and Cd(I); Ni(II) complexes of N-allylthiourea and N-phenyl-N-allyl-thioureas have sulfur coordination site. In this study it is found that the type of anion has a profound influence on the structure assumed by the complex and the coordination number which seems to be determined by the nature of the anion's size, charge, electronic configuration and coordinating power. High magnetic moments of these Oh complexes were thought to be due to spin-orbit coupling which causes an orbital contribution in the 'quenched' $^4A_{2g}$ group state of Ni (II).

Several metal ion complexes of urea, thiourea, methyl urea, thioacetamide, naptu = l-(l-naphthyl)-2- thiourea, N-phenyl thiourea, N,N'-diphenyl thiourea [14-19] and some chiral ligands indicate [14] the tendency of the metal to coordinate to the organic molecule through sulfur which decreases on passing from $SC(NH_2)_2$ to $SC(NMe_2)_2$ and more heavily substituted thiourea molecules.

Metal complex studies with ligand N-(hydroxyl)-N,N-diphenyl thiourea (HONNDPTu), have not been reported. Therefore, it was thought worthwhile to investigate some transition metal complexes with this ligand and characterize them by spectral, magnetic, structural, and thermal methods [11, 20]. Thermo analytical methods involve the study of some properties of the system such as change in weight, rate of change in weight, heat evolved or absorbed or change of temperature which is measured as a function of temperature [21].

2. EXPERIMENTAL METHODS

All chemicals used are AR or GR quality – copper chloride, copper acetate, copper nitrate, copper perchlorate, nickel chloride, cobalt chloride, ferrous ammonium sulfate, acetone, ethyl alcohol, benzene, chloroform, nitrobenzene, carbon disulfide, aniline, methyl alcohol, carbon tetrachloride, pyridine, etc.

Equipment's used are Elico LI -10 model pH meter, spectrophotometer 106 (MK II) supplied by Systronics, Toshniwal magic eye conductivity bridge with sensitive eye detector at RT and Guoy's balance, with mercury cobalt tetrathiocyanate as the calibrant [22]. It is easily prepared [23] and has a definite composition and packing properties, with accurately known susceptibility $\chi g = 16.44 \times 10^{-6}$ cgs units at 20 ^oC. Diffuse reflectance spectra were measured for solid metal complexes on Carl – Zeiss USU – 2P spectrophotometer. Magnesium carbonate was used as a reference material and as a diluent for the complex prepared by copper acetate. IR spectrophotometer 283 and Beckman's IR-20 spectrophotometer in KBr & nujol mull were used to measure the infra-red spectra of the ligand and metal complexes. Electron Spin Resonance spectra were recorded on JEOL-FE3X Electron

Spin Resonance spectrophotometer. Thermogravimetric analysis (TGA) is carried out by the dynamic thermogravimetric method.

2.1 Preparation of N-(hydroxyl)-N, N-diphenyl Thiourea

The ligand, N-(hydroxyl)-N, N-diphenyl thiourea, was prepared in three steps (11 with references therein). Phenyl isothiocyanate (C_7H_5NS) [24] and beta-phenyl hydroxylamine (C_6H_7NO) were prepared [25] and the condensation product ($C_{13}H_{12}N_2OS$) (50g) was obtained (26) in ethereal solution after refluxing for 2-3 hours to ensure a complete reaction. The product obtained was crystallized from alcohol and purity of the sample was confirmed from the elemental analysis, the melting point, and electronic spectra, Fig 1.

2.2 Preparation of Metal Complexes

2.2.1 Iron(II), Nickel(II) and Cobalt (II) complexes

Equimolar or 2:1 ligand: metal salt solution was dissolved in minimum quantity of ethyl alcohol separately (80:20 ethyl alcohol-water for iron), ligand solution was added to the metal salt solution with constant stirring, adjusted to pH 5.2 for iron, 7.8 for nickel equimolar, 5.1 for nickel 2:1, 7 for copper. On standing, puce or purplish-brown iron, green nickel, reddish-brown nickel and red-brown cobalt complexes were precipitated, filtered under suction, washed with solvent, and dried at 80-100^{o}C.

2.2.2 Copper (II) Complexes

Equimolar ligand and metal chloride or perchlorate or acetate salts and copper nitrate:ligand in 1:2 ratio, were dissolved separately in ethyl alcohol (copper nitrate with 25:75 water-ethyl alcohol), ligand solution was added slowly to the solution of metal salt with constant stirring, adjusted to pH 7.8, 7.5 for acetate. On standing, green copper chloride, light green copper perchlorate, dark brown copper acetate and brownish-green nitrate complexes were separated. They were filtered under suction, washed with the solvent, and dried at 80^{o}C. Copper nitrate complex was found insoluble in the most common organic solvents and water. Hence, it could not be crystallized.

2.3 Nitrogen and Metal Ion Analysis

Copper by the dipyridine dithiocyanate method, nickel by the nickel dimethyl glyoximate method, ferrous ion by volumetric analysis, using diphenylamine indicator, cobalt by cobalt tetrapyridine dithiocyanate method [26], nitrogen content by Duma's combustion method [27] were estimated.

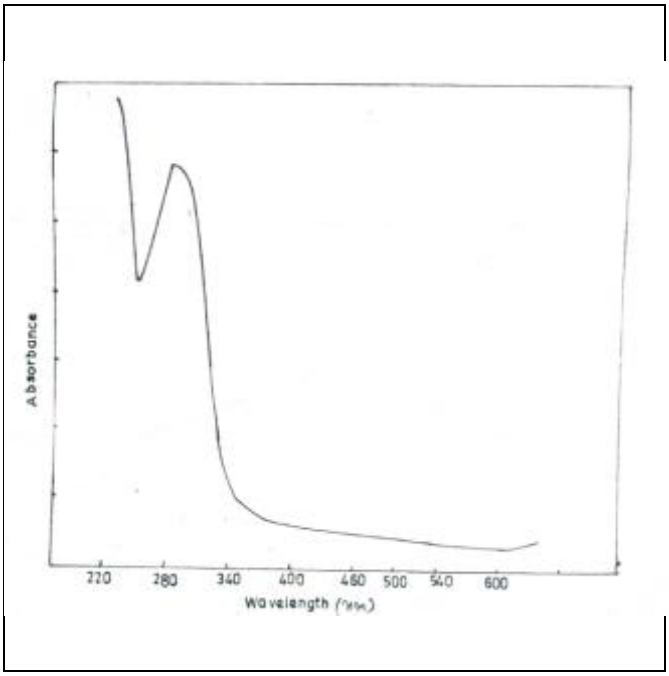

Fig. 1. Electronic absorbance spectra of Reagent

2.4 Composition of Copper (II) with Ligand in Solution

It was found that copper (II) chloride, acetate, perchlorate, and nitrate formed green, dark-brown, light-green, and brownish-green colored complexes with ligand in solution respectively. Conductivity titrations were carried out for all four complexes, rest of the other colorimetric methods were carried out by taking copper(II) chloride as representative, as they all formed from equimolar solutions identically.

In solution, metal does not absorb beyond 480 nm, the ligand does not absorb beyond 400 nm, however, the copper complex absorbs appreciably at 470 nm. Therefore, calorimetric measurements were carried out using a 470 nm filter. Effect of pH [28], Vosburgh and Cooper method [29] to confirm the presence of only one complex under the experimental conditions, Job's continuous variation method [30] to study the composition of copper (II) complex, mole ratio method [28] to indicate the presence of 1:1 species of the complex in solution and conductivity titration [31] to establish complex formed with salts of chloride, acetate, and perchlorate exist in 1:1 composition with conductance breaking at the center and for complex formed with nitrate in 1:2 composition, with the conductance break occurring with double the amount of ligand solution.

3. RESULTS AND DISCUSSION

Table 1 shows the preparation and formation of Cu(II), Ni(II), Co(II), and Fe(II) complexes, their chemical analysis. Table 2 shows the solubility's (g/L) of ligand and metal complexes. Table 3 shows the important infrared frequencies and diffuse reflectance (for the solid insoluble complexes) electronic spectral bands of the ligand and its metal complexes. Fig 2 - 10 for IR spectra and Fig 11 – 18 plotted using tables – Table 4 - 11 for diffuse reflectance spectra are available as Supplementary Material. Table 12 shows the calculations of χ_M values by applying Bleaney-Bower's equation [32] to the best fit values of J and g for the dimeric Cu(II) complexes.

3.1 Ligand

The synthesized N-(hydroxyl)-N, N-diphenyl thiourea (HONNDPTu) ligand obtained was crystallized from alcohol and purity of the sample was confirmed from the elemental analysis, the melting point. It was completely soluble in absolute ethyl alcohol, acetone and to a large extent in 25:75 water-ethyl alcohol medium. It was insoluble in chloroform, CCl_4, and benzene. Electronic spectrum of the ligand in nujol mull consists of a strong band at 285nm which could be attributed to π-π* transition.

The IR spectrum of the ligand are characterized by symmetric and anti-symmetric √NH modes (√1 and √2) usually observed [33] around 3300-3200 cm^{-1} are found at 3210 and 3140 cm^{-1}. The sharp band at 3340 cm^{-1} is assigned to √OH vibrations. As is reported for secondary thioamides [35,36], the symmetric √C-N mixed mainly with √NH bending was at 1530 cm^{-1} and the asymmetric √C-N at1520 cm^{-1}, the ligand synthesized also shows similar spectra. Symmetric √N-C=S and √C=S group vibration bands at 1230 and 760 cm^{-1} could be assigned to √C=S coupled with ring deformation as has been observed and reported (11 with references therein) to occur around 1270-1224 cm^{-1} and 785-750 cm^{-1}. The fundamental due to √C=S bonding may be attributed at 340 cm^{-1} and √C=S out-of-the-plane bending at 210 cm^{-1}, in agreement with the corresponding bands at 343 and 190 cm^{-1} in ethylene thiourea [33] and thiozolidine-2 thione [37]. A strong or medium intensity band around 1300-1200 cm^{-1} is reported [38] to be assigned to the √N-OH group and is found at 1260 cm^{-1} in the current ligand. √NH out-of-the-plane bending can be assigned to a band at 695 cm^{-1} in conformity with assignment made [40] in ethylene thiourea. It could, however, also be assigned to a forbidden √NH bending mode of (A2 symmetry) overlapping with the (B2) fundamental due to ring formation [33]. After having ascertained the composition of the ligand, the metal complexes are prepared.

Table 1. Statement showing preparation and formation of Cu(II), Ni(II), Co(II) and Fe(II) complexes, their chemical analysis

S No	Metal salt used	Complex formed	Colour observed	Metal%		Nitrogen%		μ_{eff} (BM)	Geometry
				cald	found	cald	found		
1	Fe(II)	(FeR_2H_2O)	Puce	20.30	18.84	9.64	7.72	6.3	Octahedral
2	Co(II)	$CoR_2(H_2O)_2$	Red-brown	9.97	10.00	10.00	7.51	5.8	Octahedral
3	Ni(II)	$(NiRCl)_n$	Green	10.80	10.20	10.28	11.57	4.4	Tetrahedral
4		(NiR_2)	Reddish-brown	17.41	18.28	8.30	7.54	Dia	Square-planar
5	$CuCl_2$ at pH 7.8	$(CuRCl)_2$ Dried at 80°C	Green	18.58	18.20	8.19	8.21	1.4	Dimeric square-planar
6	$Cu(ClO_4)_2$ at pH 7.5	$(CuRClO_4)_2$ Dried at 80°C	Light green	20.73	21.15	4.56	3.08	1.4	Dimeric square-planar
7	$Cu(ac)_2$ at pH 7.5	$(CuR)_2$ Dried at 80°C	Dark brown	11.19	11.15	9.86	9.11	1.3	Dimeric square-planar
8	$Cu(NO_3)_2$ at pH 7.5	(CuR_2H_2O) Dried at 100°C	Brownish green	15.65	15.22	9.81	9.86	1.9	Distorted octahedral

R = ($C_{13}H_{11}N_2OS$ – C% obs (cald) - 63.68 (64.84); H% - 5.24 (4.97); & N% = 4.96 (4.97)) with a loss of proton; Dia - Diamagnetic

Table 2. Statement showing solubility's (g/L) of ligand metal complexes

Solvent	$[CuRCl]_2$	$[CuRClO_4]_2$	$[CuR]_2$	$[CuR_2H_2O]$	$[NiRCl]_n$	$[NiR_2]$	$[CoR_2(H_2O)_2]$	$[FeR_2(H_2O)]$
Methanol	1.76	0.12	0.66	1.60	2.40	1.36	0.60	-
Ethanol	2.44	0.12	0.72	0.98	2.60	1.96	2.60	-
Chloroform	1.56	0.08	0.26	1.00	2.60	1.56	2.32	-
Carbon tetrachloride	0.12	-	0.46	0.80	2.12	1.36	3.40	-
Benzene	0.74	0.14	0.66	0.12	2.40	1.36	0.60	0.76
Pyridine	6.14	3.60	1.86	2.00	2.60	15.36	2.60	-

Table 3. Statement showing important infrared frequencies and diffuse reflectance (for the solid insoluble complexes) spectral bands in HONNDPTu and its metal complexes

R= HONNDPTu	$[CuRCl]_2$ $[CuRClO_4]_2$	$[CuR]_2$	$[CuR_2H_2O]$	$[NiRCl]_n$	$[NiR_2]$	$[CoR_2(H_2O)_2]$	$[FeR_2(H_2O)]$	Frequency
3340	-	-	3530	-	-	3530	3510	√OH stretching/ coordinated water
3210	3210	-	3210	3200	3210	3210	3210	Symmetric & anti-
3140	3140		3140	3040	3140	3140	3140	symmetric √NH vibrations
1530	1580	1550	1580	1550	1580	1580	1580	Symmetric √N-C=S
1230	1300	1280	1310	1280	1310	1310	1280	
760	750	750	750	755	750	750	750	Symmetric √C=S
1260	1230	1230	1230	1230	1230	1230	1230	Stretching √N-O
-	505	510	505	490	490	490	490	M-O bonds
-	320	300	320	350	380	330	350	M-S bonds
-	-	550	-	-	-	-	-	M-N bonds
	$[CuRClO_4]_2$	-						**Bands**
285b	360	-	340s	350-400	400	340	330s	Charge transfer bands
-	800	-	900-1000 b	700	740	680	540 (hump)	Bands characteristic
-	-	-	-	-	-	1200	1000b	of complexes

Table 12. A Table showing the calculations of χ_M values by applying Bleaney-Bower's equation with the best fit values of J and g for the dimeric Cu(II) complexes

Compound	g	J	$e^{J/kT}$	$\chi_M \times 10^{-6}$	
				calcd	expt
$[CuRCl]_2$	2.05	260	3.42	877.09	878.75
$[CuRClO_4]_2$	2.07	304	4.44	796.41	797.55
$[CuR]_2$	2.07	245	3.33	926.62	927.35

$\chi_M = N\beta^2g^2/3kT\ [1+1/3\ e^{-J/kT}]^{-1} + N\alpha$

$N\beta^2/3k = 1/7.9971$; $N\alpha = 60 \times 10^{-6}$ cgs units; $kT = 203.64\ cm^{-1}mole^{-1}$; $T = 293\ ^oK$

3.2 Assignment of Geometrical Structure based on the Complex Formation, Colour, Magnetic Moments, Electronic Spectra, Diffuse Reflectance Spectra and IR Spectra

3.2.1 Fe(II) complex $[Fe(C_{13}H_{11}N_2OS)_2H_2O]$ or $[FeR_2H_2O]$

Puce or purplish-brown Fe(II) complex has been formed with a loss of a proton from ligand. This decomposes in solvents, water and in the presence of moisture. It is paramagnetic with μ = 6.3BM, indicating it to be high spin Oh complex [34].The electronic spectra of this complex consist of only the $^5T_{2g}$ to ^5E_g transition which is reported to occur at 1000nm. Diffuse reflectance spectrum of Fe(II) complex showing a strong band around 330nm could be assigned to π-π* transition in the ligand, a hump at 540nm, a charge-transfer transition and a broad band at 1000nm attributed to $^5T_{2g}$ to ^5E_g transition in the complex (11 with references therein).

On the basis of the observed magnetic and spectral properties, Fe(II) complex could be represented by the possible Structures – 1-3.

3.1 Ligand

The synthesized N-(hydroxyl)-N, N-diphenyl thiourea (HONNDPTu) ligand obtained was crystallized from alcohol and purity of the sample was confirmed from the elemental analysis, the melting point. It was completely soluble in absolute ethyl alcohol, acetone and to a large extent in 25:75 water-ethyl alcohol medium. It was insoluble in chloroform, CCl_4, and benzene. Electronic spectrum of the ligand in nujol mull consists of a strong band at 285nm which could be attributed to π-π* transition.

The IR spectrum of the ligand are characterized by symmetric and anti-symmetric √NH modes (√1 and √2) usually observed [33] around 3300-3200 cm^{-1} are found at 3210 and 3140 cm^{-1}. The sharp band at 3340 cm^{-1} is assigned to √OH vibrations. As is reported for secondary thioamides [35,36], the symmetric √C-N mixed mainly with √NH bending was at 1530 cm^{-1} and the asymmetric √C-N at1520 cm^{-1}, the ligand synthesized also shows similar spectra. Symmetric √N-C=S and √C=S group vibration bands at 1230 and 760 cm^{-1} could be assigned to √C=S coupled with ring deformation as has been observed and reported (11 with references therein) to occur around 1270-1224 cm^{-1} and 785-750 cm^{-1}. The fundamental due to √C=S bonding may be attributed at 340 cm^{-1} and √C=S out-of-the-plane bending at 210 cm^{-1}, in agreement with the corresponding bands at 343 and 190 cm^{-1} in ethylene thiourea [33] and thiozolidine-2 thione [37]. A strong or medium intensity band around 1300-1200 cm^{-1} is reported [38] to be assigned to the √N-OH group and is found at 1260 cm^{-1} in the current ligand. √NH out-of-the-plane bending can be assigned to a band at 695 cm^{-1} in conformity with assignment made [40] in ethylene thiourea. It could, however, also be assigned to a forbidden √NH bending mode of (A2 symmetry) overlapping with the (B2) fundamental due to ring formation [33]. After having ascertained the composition of the ligand, the metal complexes are prepared.

IR spectra of KBr and Nujol mull do not show a strong and sharp absorption band in the region 3400-3300 cm^{-1} indicating that the complex does not contain a =N-OH group and that hydrogen of the N(hydroxy) group has been replaced by the metal atom in the complex formation. Structure 1 cannot account for the absence of this strong band and hence cannot be assigned. Structure 3 requires the presence of a band due to C=S and -NH coordinated to metal. Bands at 3210 and 3140 cm^{-1} due to symmetric and anti-symmetric √NH mode [33] in the ligand are not affected in the complex indicating that -NH group has not coordinated to the metal in the complex formation. However, the band at 760 cm^{-1} has been shifted to 750cm^{-1} indicating the participation of C=S in the complex. In view of these findings, Structure 3 cannot be assigned as the probable structure of Fe(II) complex.

These spectra are compared with well characterized dialkyl phenyl substituted thioureas [41,42] to ascertain the mode of bonding from the ligand to the metal ion. It was observed that on sulfur coordination, the bands around 1515 and 1280 cm^{-1} increase by about 25-30 cm^{-1} and the band at 770 cm^{-1} decrease by about 10 cm^{-1}, while on nitrogen coordination the shifts are in the reverse order [43]. In this complex, the bands assigned to √N-C=S are found shifted to 1580 cm^{-1}, 1280 cm^{-1} while the √C=S band shifted downwards to 750 cm^{-1}. These observations are in conformity with Structure 2 that the coordination to the metal is through sulfur of the keto group in the ligand.

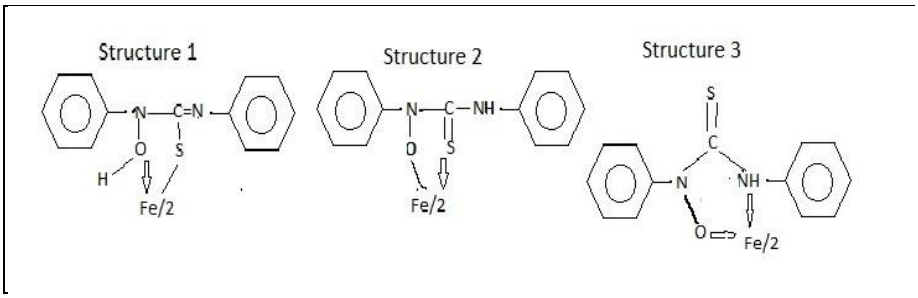

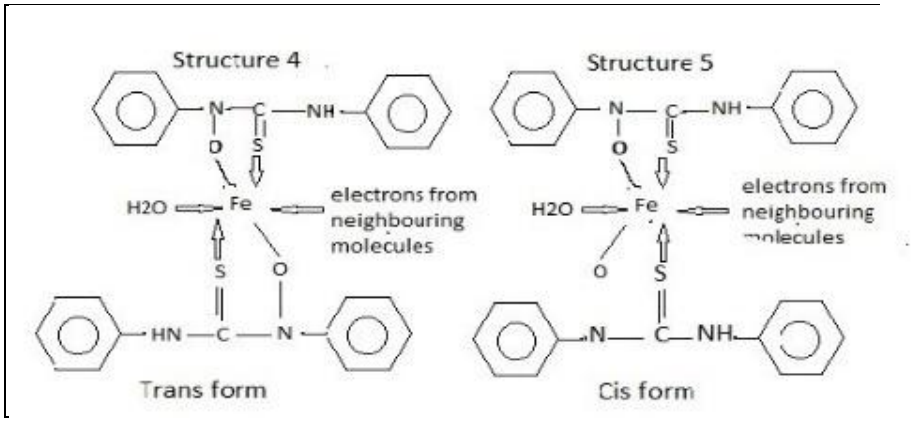

Structures 1-5. Proposed Structures for Fe(II) complex formed

Structure 2 implies that the complex should exhibit a band due to √N-O stretching frequency found as a strong band at 1260 cm^{-1} in the ligand. In this structure, the bonding to the metal through oxygen of N-O group results in the double bond character of N-oxide and so lowering of its frequency to 1230 cm^{-1} in the complex. This also requires the presence of bands due to M-O and M-S linkages, thus the new bands at 490 and 350 cm^{-1} confirm the same (11 and references therein). And the presence of a band due to the coordinated water molecule which is confirmed by, the strong band at 3510 cm^{-1} in the complex and the weight loss corresponding to a water molecule in TG curve. These findings suggest that Fe (II) complex may be represented by either of the Structures 4-5 which satisfy all requirements as observed. Steriochemically trans form is more stable than the cis form. Therefore, the Fe (II) complex possibly attains Oh configuration by sharing electrons from the neighboring molecules and could be well represented as shown by Structure 4.

3.2.2 Co(II) complex: $[Co(C_{13}H_{11}N_2OS)_2(H_2O)$ or $CoR_2(H_2O)_2$

Red-brown Co(II) complex is very sparingly soluble and so could not be crystallized. It is found to be paramagnetic with μ = 5.8BM, indicating it to be a high spin Oh Co (II) complex, which range from μ = 4.7-5.5BM [44], because of the high orbital contributions, since the spin moment only for the unpaired electrons is only μ = 3.89BM. This high orbital contribution is attributable to three-fold orbital degeneracy of $^4T_{1g}$ ground state. Due to poor solubility, instead of electronic spectra, diffuse reflectance spectra are recorded indicating visible bands which are weak and placed in the blue part of the spectrum, thus accounting for red-brown color of aquo Co(II) ions. Absorption band around 1200 nm for Co(II) Oh complex would arise due to $^4T_{1g}$ (F) to $^4T_{1g}$ (P) transition on the high frequency side as a consequence of spin-orbit coupling in the $^4T_{1g}$ (P) state based on energy-level diagram for a d^7 Co(II) ion in an Oh field (11 and references therein),but could not be observed. While a band due to $^4T_{1g}$ (F) to ^2A_gtransition is observed at 680nm in the diffuse reflectance spectra of the complex. On the basis of magnetic and spectral data, Co(II) complexes could be represented by Structures 6 and 7.

IR spectrum of Co(II) showed presence of a sharp peak at 3530 cm^{-1} which could be allotted to the coordinated water molecules. The thermogram showed a curve due to the weight loss corresponding to two water molecules

conforming the same. The bands assigned to the symmetric and asymmetric modes of √NH [33] are not affected by the complex formation. The bands due to √N-C=S are shifted to higher frequency at 1580 and 1310 cm^{-1} respectively indicating the participation of C=S in the complex formation. The band due to C=S has shifted downwards to 750cm^{-1} in the complex. The band of N-O shifted to lower frequency at 1230 cm^{-1} in the complex indicating the formation of M-O bond through O of N-O resulting in the double bond character of N-O. Two new bands at 490 and at 330 cm^{-1} appear in the complex and are assigned to M-O and M-S bonds, respectively [11 and references therein].

From the above observations, it is concluded that Co(II) complex is an Oh high spin complex and can be represented as in Structure 6 as a trans type which explains the presence of all observed bands in the IR spectrum as well.

3.2.3 Ni(II) complex

Green 1:1 Ni(II) complex is paramagnetic with μ = 4.4BM, insoluble in the most common organic solvents and water indicating its polymeric character. The magnetic moment with μ = 3.5-4.5BM, due to very high orbital contributions [44] from degenerate ground states resulting in the built up of high magnetic moment, indicating probable Td structure. Due to poor solubility instead of electronic spectra, diffuse reflectance spectra recorded show two bands, one around 700nm and the other between 350-400nm, which is assigned to $T_1(F)$ to T1(P) transition and $T_1(F)$ to A_2 transition respectively. These are characteristic of Td Ni(II) complexes (11 and references therein), generally attributable to charge transfer, absorption tailings in the visible to UV region.

The IR spectra shows the √N-C=S bands shifted to 1550 and 1280 cm^{-1}, the band assigned to √C=S has shifted to lower frequency 755 cm^{-1}. The observed bands are in conformity with the coordination through sulfur. Structure 8 indicates N-oxide coordinated to metal through O resulting in the double bond character of N-O with a lowering in the bond frequency to 1230 cm^{-1} in the complex. The bands at 490 $cm^{-1}$and 350 cm^{-1} are allotted to M-O linkage and M-S in the complex formation (11 and references therein).Two bands 3200 and 3040 cm^{-1} are assigned to the symmetric and antisymmetric frequencies of √NH indicate the coordination of this group to metal. The thermogram shows that the decomposition reaction to be of simultaneous nature leading to NiS as the residue confirming with the molecular formula $[NiRCl]_n$. On the basis of the above evidences, the green Ni(II) complex is Td, with M-M interaction in the polymeric form.

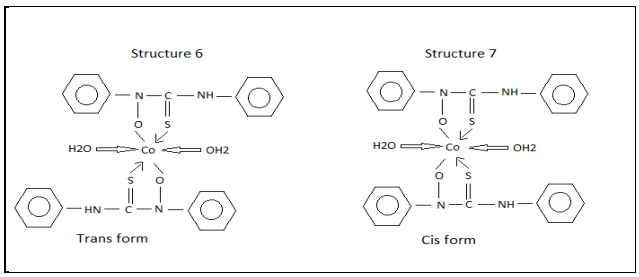

Structures 6-7. Proposed Structures for Co(II) complex

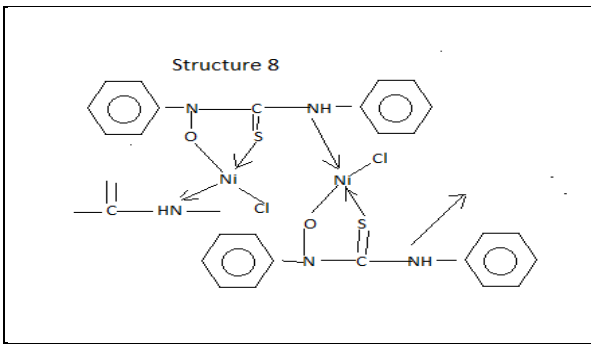

Structure 8. Proposed Structure for Ni(II) complex

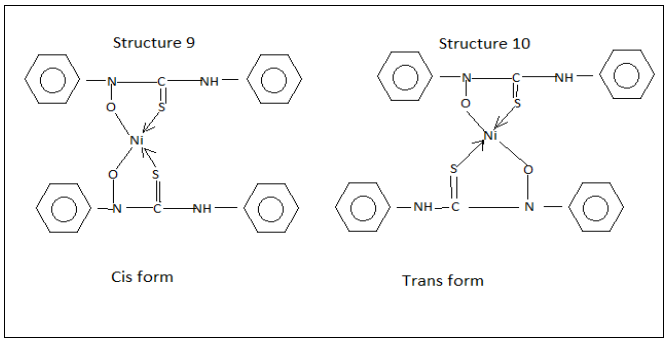

Structures 9-10. Proposed Structure for Ni(II) complex

Lustrous reddish-brown Ni(II) complex is moderately soluble in the most common organic solvents and fairly well soluble in pyridine. It is diamagnetic in nature and indicates that it is a square-planar [38,39] four coordinate Ni(II) complex, involving dsp^2 hybridisation.

The diffuse reflectance spectra in the solid state exhibits two bands at 740nm and 400nm. The position and intensity of the band at 740nm indicate that it has characteristic features of d-d transition bands in a neutral, spin-paired, diamagnetic, square-planar structure with ground state $^1A_{1g}$. Based on d-orbital energy level diagram in square planar nickel complexes, the band at 740nm may be assigned to the first spin-allowed transition $^1A_{1g}$ to $^1A_{2g}$ (11 and references therein).

IR spectrum of this complex does not show any band for √OH group indicating the proton in the hydroxylamine group of the ligand being replaced by the metal atom in the complex formation. √NH bands also are not affected in the complex formation. Double bond character of N-oxide linked to M-O shows strong band at 1230 cm^{-1}. The strong bands at 490 and 380 cm^{-1}, are assigned to M-O and M-S bonds, respectively (11 and references therein).

The observed bands at 1580 cm^{-1}, at 1310 cm^{-1}, at 750cm^{-1} are in conformity with the coordination through S in the present substituted thiourea Ni(II) complex. On the basis of these data, it can be concluded that the lustrous reddish-brown Ni(II) complex is square-planar and can be represented as shown in Structure 10, which is a trans form considered more stable than the cis form as in Structure 9 and satisfies all characteristic features required.

3.2.5 Copper complexes

Cu(II) complexes were prepared by reacting chloride, perchlorate, acetate, and nitrate salts. They are found to be highly insoluble or very slightly soluble in the most common organic solvents and water, they could not be crystallized. Elemental analysis was checked to ascertain the purity and the molecular formulae of the complexes. The magnetic and spectral properties of these complexes have been studied and the results are utilized to propose the structure of these complexes, for green $[CuRCl]_2$, light green $[CuRClO_4]_2$, dark brown $[CuR]_2$ and brownish green $[CuR_2H_2O]$ complexes.

3.2.5.1 Composition of the Cu(II) complexes - Studies in solution

On adding alcoholic solutions of ligand and copper salt, with chloride, perchlorate, acetate, and nitrate, shades of green colour developed in each case. Therefore, a colorimeter was used to determine the nature of the composition of the complexes formed in solution.

Cu(II) chloride was studied as a representative since the solution studies for all three Cu(II) complexes would be experimentally identical as they are 1:1 complexes.

Detailed solution studies of green Cu(II) chloride complexes are discussed:

(a) Study in solution

pH studies of the complex and ligand in 1:1 ratio, in 25ml flasks with varying amounts of solutions, by adding dilute ammonia, pH and absorbance were measured. The pH vs absorbance curve shows the complex formation at the pH range 7.5-8.0 along with satisfactory colour stability or the optical density of the system nearly remaining the same and hence all solution studies were made at 7.8, Fig. 19, Table 13

Table 13. Effect of pH on absorbance of $Cu(C_{13}H_{11}N_2OS)Cl$ Concentration of copper chloride & ligand: 1 x 10^{-3}M; Filter – 470 mμ; Solvent – ethyl alcohol

S.No	pH	Absorbance
1	2.4	0.014
2	3.4	0.017
3	5.0	0.020
4	7.3	0.026
5	7.9	0.027
6	8.1	0.027
7	8.3	0.027
8	8.4	0.027
9	8.7	0.027
10	9.0	0.028
11	9.5	0.029

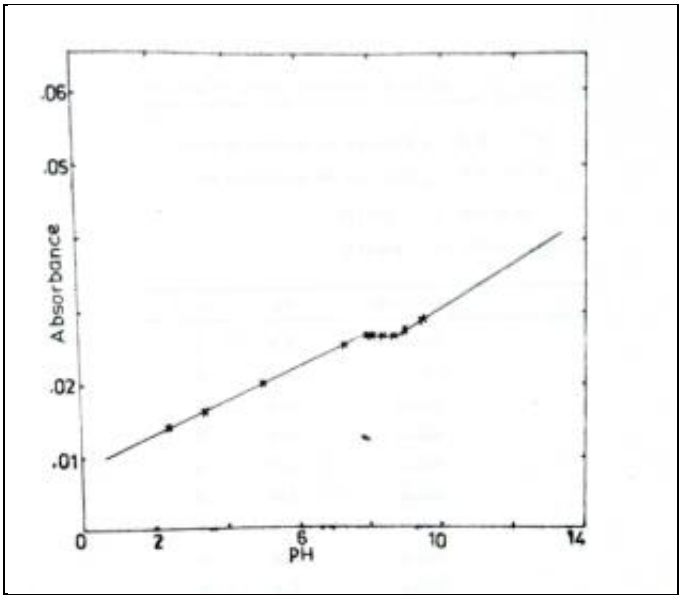

Fig. 19. Effect of pH on absorbance of Cu(II) complex in alcohol solvent

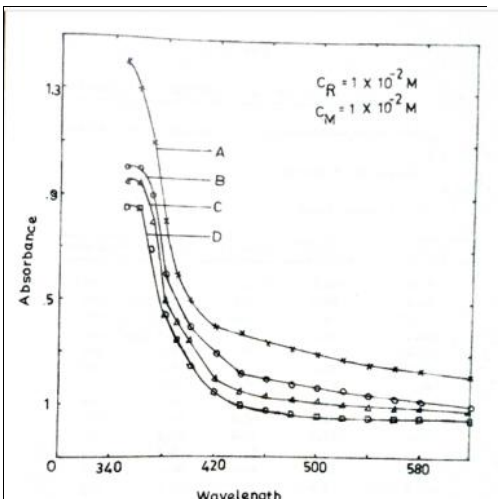

Fig. 20. Method of Vosburgh & Cooper for CuRCl complex (A-1:1, B-1:2, C-1:3, D-1:4)

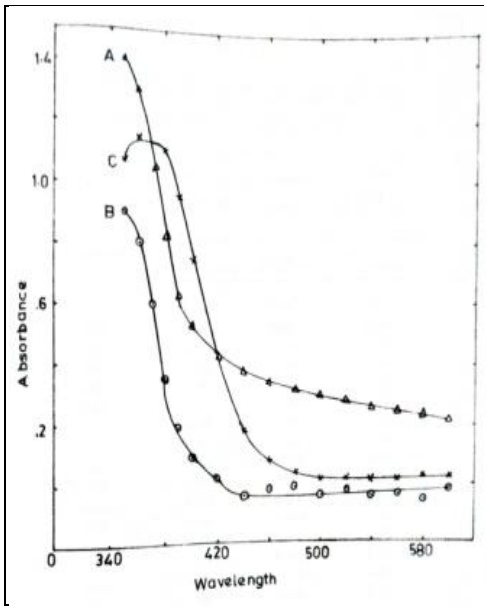

Fig 21. Absorbance of A-CuRCl, B-Reagent and C-$CuCl_2.2H_2O$

Table 14. Vosburgh and Cooper method of $Cu(C_{13}H_{11}N_2OS)Cl$ Concentration of copper chloride & ligand: 1 x 10^{-2}M Solvent – ethyl alcohol; Total Volume: 10-25 ml

Wavelength	Absorbance			
	1:1 (M:R)	1:2 (M:R)	1:3 (M:R)	1:4 (M:R)
350	1.4	1.0	0.95	0.85
360	1.3	1.0	0.95	0.65
370	1.1	0.9	0.8	0.7
380	0.8	0.6	0.5	0.45
390	0.6	0.5	0.42	0.35
400	0.5	0.4	0.35	0.25
420	0.4	0.3	0.2	0.15
440	0.38	0.22	0.15	0.1
460	0.34	0.2	0.14	0.08
480	0.32	0.18	0.12	0.07
500	0.30	0.17	0.11	0.06
520	0.28	0.16	0.11	0.05
540	0.26	0.14	0.1	0.05
560	0.25	0.13	0.1	0.05
580	0.24	0.12	0.1	0.05
600	0.22	0.11	0.09	0.05

Table 15 Absorbance Spectra of HONNDPTu, $CuCl_2.2H_2O$ and $[Cu(HONNDPTu)Cl]_2$ in Ethyl alcohol C_M = 1x10^{-2}M and C_R= 1x10^{-2}M

Wavelength	Metal absorbance	Reagent absorbance	$[Cu(HONNDPTu)Cl]_2$ absorbance
350	1.07	0.9	1.4
360	1.15	0.8	1.3
370	1.13	0.6	1.04
380	1.10	0.35	0.82
390	0.95	0.19	0.63
400	0.75	0.09	0.53
420	0.43	0.02	0.43
440	0.18	0.004	0.38

460	0.08	0.002	0.34
480	0.04	0.001	0.32
500	0.02	0.004	0.30
520	0.02	0.002	0.28
540	0.01	0.004	0.26
560	0.02	0.003	0.25
580	0.03	0.005	0.4
600	0.03	0.001	0.22

(b) Vosburgh and Cooper method

Absorption curves obtained with varying M:L ratio – 1:1, 1:2, 1:3, 1:4 molar proportions at pH 8.0, are similar in shape throughout the range and do not differ from the one with an excess of ligand. Thus, the curves do not show any maxima or shoulder, indicating that only one absorbing species of the metal complex is present in the solution. Absorption spectra of copper salts show minimum absorption at 470mm, while that of Cu(II) complex has a very strong absorption at this wavelength, hence all colorimetric measurements were made at 470nm. Fig. 20 and Fig 21, Table 14 and Table 15.

(c) Job's continuous variation method

The curves obtained by plotting the absorbance against the volume of $CuCl_2.2H_2O$ solution at 470nm indicate a maxima at a volume of 5ml, with the mole fraction of Cu(II) to that of the ligand as 1:1, for a series of solutions in which the ratio to metal varied from 1:9 to 9:1, Fig 22, Table 16 given .

Table 16. Composition of Cu (II) complex by Job's method Solvent: Ethyl alcohol; Total volume of Cu(II) + reagent: 10 ml; Filter 470 mμ

Volume of Cu(II) in ml	Volume of reagent in ml	Absorbance	
		A= $C_R=C_M$ = 1x10^{-3}M	B= $C_R=C_M$=1x10^{-2}M
0	10	0.01	0.07
1	9	0.02	0.08
2	8	0.05	0095
3	7	0.07	0.11
4	6	0.08	0.124
5	5	0.08	0.112
6	4	0.07	0.101
7	3	0.06	0.086
8	2	0.05	0.070
9	1	0.04	0.065
10	0	0.03	

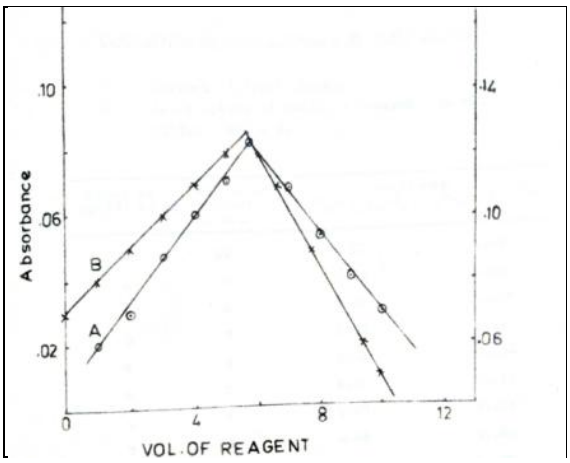

Fig. 22. Composition of CuRCl – Job's method for C_R & C_M – A-1x10^{-2} & B-1x10^{-3}

(d)Mole ratio method

The linear parts of the curves obtained in this case, intersect at 1:1 value, with a sharp break, of the mole ratio of M:R, Fig 23, Table 17 as given.

Table 17. Composition of Cu(II) complex by Mole Ratio Method Solvent: Ethyl alcohol; Total Volume: 8 ml; Filter: 470 mμ

Mole of reagent per mole of Cu(II) ion	Absorbance	
	$C_R=C_M = 1x10^{-2}M$	$C_R=C_M = 1x10^{-3}M$
4.0	0.06	0.008
3.0	0.08	0.005
2.3	0.07	0.006
1.8	0.08	0.010
1.5	0.08	0.006
1.2	0.075	0.006
1.0	0.08	0.010
0.8	0.075	0.003
0.6	0.07	0.004
0.5	0.066	0.003
0.4	0.06	0.004
0.3	0.07	0.003
0.2	0.07	0.005

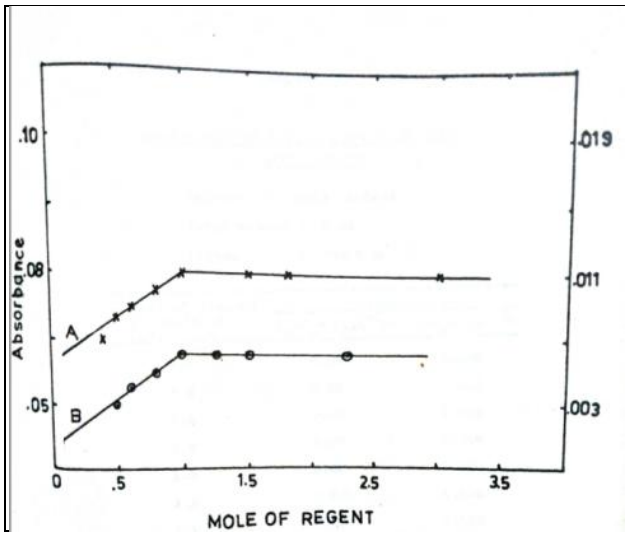

Fig. 23. Composition of CuRCl – Mole Ratio method $A=C_R=C_M = 1x10^{-2}$; $B=C_R=C_M=1x10^{-3}$

(e) Conductometric titration

Formation of the complexes with all salts reveal that Cu(II) exists in 1:1 composition in all cases except in the case of Cu(II) nitrate complex, where it is in 1:2 mole ratio, confirming the results obtained from mole ratio method and Job's continuous variation method. The species of the Cu(II) complex in solution may probably be represented as $[CuR^+]$ or [CuR+X-], where X^- stands for Cl^- and ClO_4^-, Fig 24-27 & Table 18-as given.

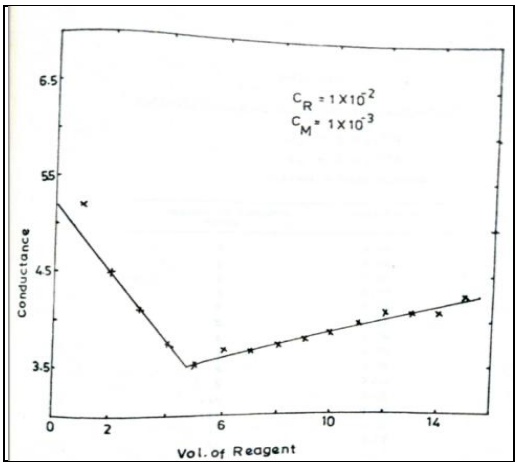

Fig 24. Composition of CuRCl-Conductometric titration

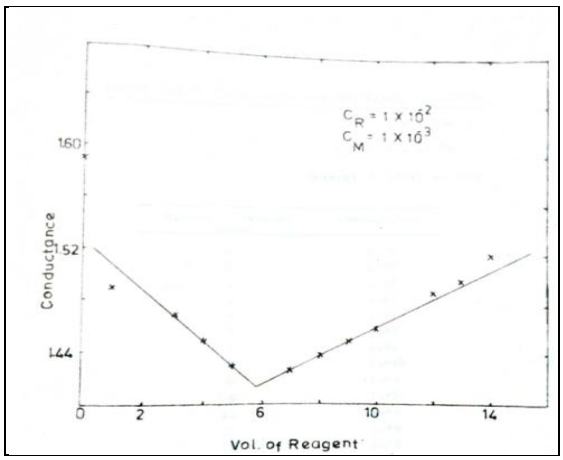

Fig. 25. Composition of $CuRClO_4$-Conductometric titration

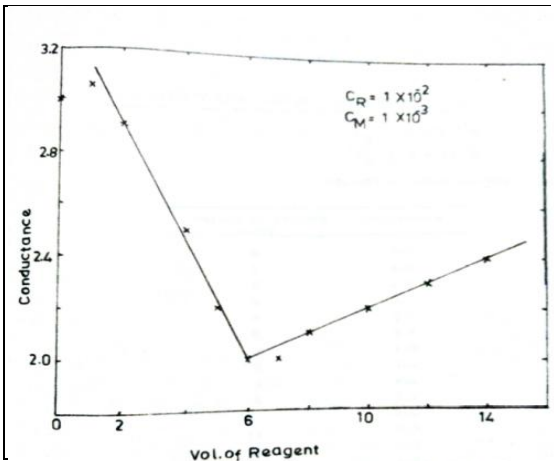

Fig. 26. Composition of $(CuR)_2$-Conductometric titration

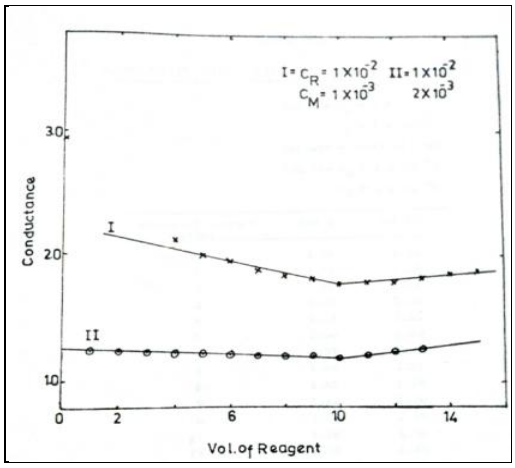

Fig. 27. Composition of CuR_2H_2O-Conductometric titration

Table 18. Conductivity Titration Cu(II) salts and Ligand Solvent: Ethyl alcohol; C_M = 1x10^{-3}M and C_R= 1x10^{-2}M; Set II C_M = 1x10^{-3}M and C_R= 2x10^{-3}M

Volume of reagent added	Conductance (CuRCl)	Conductance $Cu(R)ClO_4$	Conductance $Cu(R)_2$	Conductance of $Cu(R)_2H_2O$	
				Set I	Set II
0	6.65	1.59	3.0	2.94	1.28
1	5.26	1.49	2.9	2.56	1.25
2	4.55	1.47	2.9	2.38	1.24
3	4.17	1.47	2.8	2.27	1.23
4	4.00	1.45	2.5	2.13	1.22
5	3.51	1.43	2.2	2.00	1.22
6	3.70	1.41	2.0	1.97	1.21
7	3.70	1.425	2.0	1.88	1.21
8	3.75	1.44	2.1	1.85	1.20
9	3.80	1.45	2.2	1.82	1.20
10	3.85	1.46	2.2	1.78	1.19
11	4.00	1.49	2.3	1.78	1.20
12	4.17	1.49	2.3	1.78	1.22
13	4.17	1.50	2.4	1.82	1.24
14	4.17	1.52	2.4	1.85	-
15	4.35	-	-	1.88	-

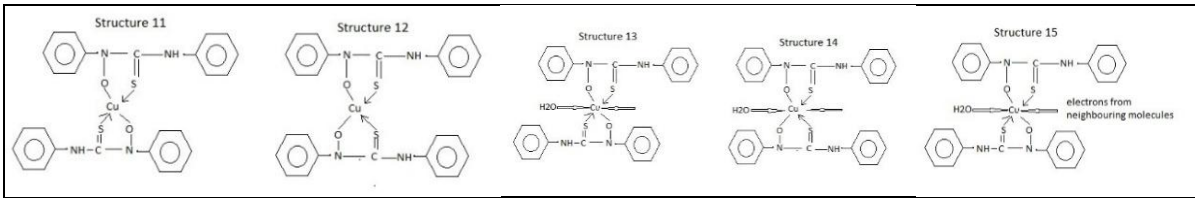

Structures 11-15. Proposed Structures for Cu(II) complex

3.2.5.2 CuR_2H_2O complex

This brownish-green complex shows μ=1.9BM at RT, which is in agreement with that expected for one unpaired electron, 1.78BM observed for Oh Cu(II) complexes. Diffuse reflectance spectra of this complex show two peaks. A strong and sharp peak is at 340nm and a broad band is noticed in the range 900-1000nm. The former peak is attributed to π-π* transition in the ligand,

the broad band beginning from 900nm may be due to d-d transition usually found to be present in octahedral (Oh) or distorted Oh, Cu(II) complexes and represented as shown in Structures 11,12.

However, from the IR spectra, appearance of a new strong, sharp band at 3530 cm^{-1} in the complex indicates the presence of coordinated water after the complex formation and absence of the band at 3340 cm^{-1} indicates replacement of hydrogen in N-OH group by the metal in the complex formation. This observation is in conformity with the results thermogram of the complex showing weight loss corresponding to one molecule of water, agreeing with the proposed molecular formula $[CuR_2H_2O]$. Hence it is represented as in Structures 13,14 containing a coordinated water molecule.

These structures require the presence of bands due to the coordination of the M-S of the C=S group and coordination to M-O of N-oxide group. IR spectrum of the complex did not show any change in the bands indicating that the –NH group does not participate in the complex formation. Spectra of the complex show that the bands due to √N-C=S have shifted slightly upwards to 1580 and 1310 cm^{-1} respectively and the band due to √C=S is slightly shifted to to 750 cm^{-1} indicating the participation of C=S. The band at 1230 cm^{-1} in the complex, confirms the participation of N-oxide group. The new bands found in the complex at 505 cm^{-1} and 320 cm^{-1} are assigned to M-O and M-S vibrations, respectively. The IR spectrum satisfies all requirements for the distorted Oh, as indicated in the cis and trans Structures 13,14. As Oh environment of Cu(II) complex is achieved by coordination through the nitrogen atoms of the neighbouring molecules leading to the polymetric nature of the complex and so, the distorted Oh Cu(II) complex is better represented by Structure 15.

Complexes formed from chloride, perchlorate, and acetate salts are found to show sub-normal magnetic moment at RT, so probably polymeric or dimeric in nature, and so in agreement and conformity with the observed insoluble character of the complexes. They could be represented as $(CuRCl)_2$; $(CuRClO_4)_2$; and $(CuR)_2$. They form 1:1 complexes with the ligand with a loss of proton on complex formation, with an effective μ around 1.4BM (within ±1%) in each case confirmed compared to μ=1.7BM, the spin-only value expected for Cu(II) ion containing one unpaired electron. Sub normal magnetic moment is indicative of Cu-Cu interaction in the polymeric solid state. Cu(II) complexes are reported (11 and references therein) to form a large number of binuclear systems in which Cu atoms undergo antiferromagnetic interactions resulting in an abnormally low values of magnetic moment.

Binuclear Cu(II) complexes are reported to conform with Bleaney Bower's equation [32]

$$\chi_M = (N\beta^2g^2/3kT)\ [1+1/3\ e^{J/KT}]^{-1} + N\alpha \quad \ldots\ldots\ldots\ldots\ldots\ldots (1)$$

The average magnetic susceptibility per Cu ion for the Cu(II) complex in each case was computed with J, g, and Nα parameters. The average value of g, the gyromagnetic constant, was determined from the ESR spectra, using relation hv= gβH, where h = Planck's constant; β = Bohr Magneton; and H – field strength; the energy of separation between a singlet and triplet state is indicated by J. The molar magnetic susceptibility of the complexes was calculated by the best fit method using different values of J and the value of 'g' as obtained experimentally from the ESR spectra. The ESR spectra of the three Cu(II) complexes were recorded Fig. 28-30 as given in Supplementary Material. From these spectra, the value of g, Lande' splitting factor, or spectroscopic splitting factor was evaluated. These values of 'g' for the respective complexes have been recorded in Table 12. These values could be used to theoretically calculate the molar magnetic susceptibility at any given temperature. Experimental molar magnetic susceptibilities as determined at RT agree very well with the calculated values, indicating that the results are in conformity with the Bleaney Bower's equation.

Subnormal magnetic moment, applicability of Bleaney Bower's equation suggest the occurrence of association of a [CuRX] complex molecules, where X stands for chloride or perchlorate ions, by coordination of the binding S atoms to Cu(II) ions in the adjacent molecules, as has been previously observed [45] in some of the dimeric complexes containing S bridge between Cu atoms. On the basis of the above observations, the three Cu(II) complexes have binuclear structure and represented by the probable Structures 16-23. Binuclear Structures 16-19 involve a sulfur bridges between Cu(II) atoms and postulate [46] that thioketonic S is coordinated to Cu atoms.

Reflectance spectrum of the light green Cu(II) complex reveals two peaks, one around 360nm and the other at 800nm with the ratio of the optical densities very nearly equal to 2, while the green copper complex and dark-brown, exhibit two bands which are characteristic features of dimeric Cu(II) complexes. Therefore, Cu(II) complexes are considered square planar dimeric and could be represented by Structures 16,17,20 and 21.Structures 18, 19 are square pyramidal. Electronic and reflectance spectral bands for the five coordinate Cu(II) complexes are significantly different, they do not show strong antiferromagnetic character and do not have much depressed magnetic moment similar to the three Cu(II) complexes. Hence, Structures 18, 19 could not be assigned as probable structures to any of the green Cu dimeric complexes. Structures 20, 21 postulate the existence of O bridge between Cu atoms. The extent of subnormal magnetic moment as observed in the case of three Cu complexes does not warrant the assignment of these structures containing O bridges between copper atoms. Presence of an oxygen bridge between copper atoms would result in a super exchange phenomenon resulting in suppressed magnetic moment (11 and references therein). On the basis of these observations, these structures could not possibly be allotted to any of these Cu(II) complexes.

The green Cu(II) complex contains chlorine as a constituent and hence the dimeric structure can also be postulated with chloride [47] as a bridging atom between the two Cu atoms. The possible Structures are 22,23. However, it has been previously reported that dimeric Cu(II) complexes containing a chloride bridges between Cu atoms do not exhibit super exchange phenomenon and suppressed magnetic moment to a marked extent as has been observed. So does not justify these structures. In view of these characteristic spectral and magnetic properties, square planar Cu(II) dimer complexes and could be represented by either of the Structures 16,17.

IR spectra of the green Cu(II) complexes and the ligand in nujol, mull, and KBr are recorded. Complete absence of the band at 3340 cm^{-1} in the spectra of the three copper complexes gives an additional evidence in support of the assignments and suggests that the hydrogen atom of the N-OH group is replaced by Cu atom in the formation of Cu(II) complexes. The cis and trans Structures 16, 17 contain bonded thioketone groups which have shifted to higher frequency 1580 cm^{-1} and 1300 cm^{-1} in the complex and the third band to have shifted to lower frequency 750 cm^{-1}. These structures also require the presence of N-O, M-O, and M-S bonds. The band assigned to N-O frequency [38] has shifted to 1230 cm^{-1} in the two Cu(II) complexes indicating the N-O linkage to the metal atom. The new bands appearing at 505 cm^{-1} and 320 cm^{-1} in the two complexes are assigned to M-O and M-S, respectively. The steric hindrance would require the trans form to be more stable and would cause stabilization.

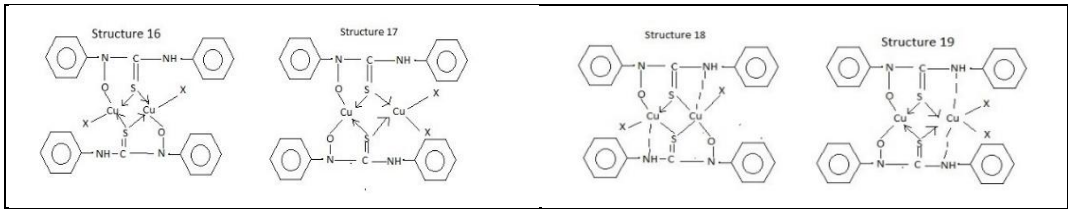

Structures 16-19. Proposed Structures for Cu(II) complexes

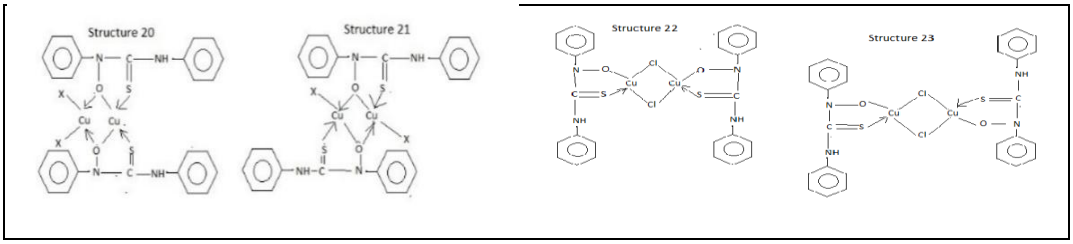

Structures 20-23. Proposed Structures for Cu(II) complexes

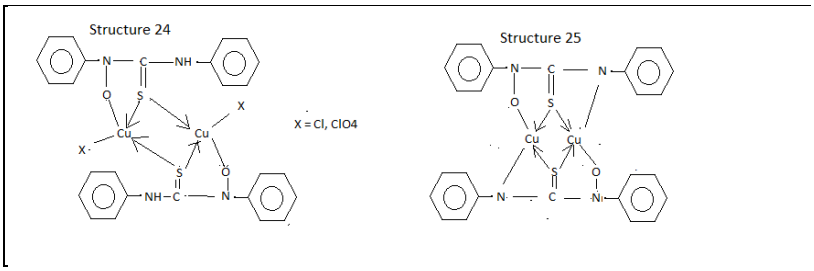

Structures 24-25. Proposed Structures for Cu(II) dimer complexes

Based on the above characteristics exhibited by the $[CuRCl]_2$ and $[CuRClO_4]_2$ complexes, the two Cu atoms bridged by S atoms of the ligand are binuclear and could be represented as $[CuRX]_2$. It satisfies all characteristics required for a four coordinate square planar binuclear Cu(II) complex which could be well represented by the trans isomer Structure 24.

3.2.5.4 Copper(II) dark-brown acetate complex

$[CuR]_2$ –acetate does not remain as a constituent of the complex. Since it is highly insoluble in the most common organic solvents and exhibits sub-normal magnetic moments, indicative of its polymeric nature leads to the consideration that the dark-brown Cu(II) complex is probably dimeric and could be represented as $[CuR]_2$ as shown in Structures 25.

It has been reported that S in thiourea complexes can form 1,2,3 coordinate bonds, i.e., itself being 2,3,4 bonded. The dark-brown Cu(II) complex represented by Structure 25 requires the presence of two coordinated S of the thioketone group and forms a bridge between Cu atoms in the complex. Presence of two coordinate S of the thioketone groups coordinating to the metal should result in the inversing of √C=S frequency to a lower level as has been reported [48].Structure 25 requires that the spectra should show bands due to bonded thioketone and all relevant bands for √N-C=S groupings. The bands of √N-C=S and √C=S in the square planar dimeric Cu complex are shifted to 1550 cm^{-1}, 1310 cm^{-1} and 750 cm^{-1}. This structure requires the presence of bands due to M-O and M-N and the absence of a band due to √NH frequency at 3200 and 3140 cm^{-1}. The spectra show bands at 510 cm^{-1}, at 550 cm^{-1} and at 300 cm^{-1} which could be allotted to M-O, M-N, and M-S, respectively. In view of these findings, the dark brown Cu(II) complex could be a square planar dimeric complex represented by Structure 25 which satisfactorily explains all spectral and magnetic properties indicated.

3.4 Thermal Studies

In the case of a mixture of calcium and magnesium carbonates, precipitated as their oxalates, the thermogram of the mixture is run [49]. It is compared with the thermograms of individual oxalates and (e) estimation of kinetic parameters (activation energy E, order of reaction n, and frequency factor z) during degradation by TGA: When two or more decomposition reactions are represented by a single TGA thermogram, where the kinetic behavior is similar at different temperatures or at different heating rates, is a condition for an isokinetic process where the reaction mechanism does not change with temperature. For this purpose, w versus tr (fraction decomposed versus reduced time) plots at different heating rates can be used safely to calculate the same (11 with references therein). These calculations indicate that thermo-analytical results and techniques, both isothermal and dynamic, may under certain conditions, be used to obtain reliable kinetic data for clearly identifiable steps in thermal decomposition. Moreover, these methods may be used to study the decomposition of both single crystal and powdered samples. Thus, a study of thermal analysis for the synthesized ligand and complexes was taken up.

3.4.1 Ligand

Thermogram of ligand and the thermogram of [the loss in the weight calculated vs % wt loss at different stages of decomposition temperature plotted against the respective temperatures], Table 19 both indicate that ligand decomposes in two steps, Fig 31, 32, as given in Supplementary Material. The loss is the first step of decomposition in T range 160-300 ^oC corresponds to $C_{12}H_{10}N_2O$, while the remaining component corresponding to H_2O decomposed in 440-560 ^oC range. The weight loss in the second step corresponds to a loss of water molecules, H_2O and S which probably gets oxidized to SO_2 and is lost.

Table 19. Showing coordinates of graphs required for Freeman and Carroll equation for ligand for evaluation of kinetic parameters

wt loss dw	dT°K	Slope values dw/dT	wr = (wc-w)	∆log wr	∆log dw/dT	Slope values ∆log dw/dT vs ∆log wr	∆ 1/T (x10^{-4})	Slope values ∆ 1/T vs ∆log wr	E and n Kcal/mole
12.5	313	1.25	75	1.87	0.09	0.4	31.96	0.14	2.3
25	313	1.25	62.5	1.79	0.09	0.48	31.96	0.3	0.35
37.5	323	1.2	50	1.69	0.07	0.5	30.96	0.5	
50	333	1.0	37.5	1.57	0.00	0.44	30.03	0.55	
58	338	1.15	25	1.39	0.06	0.5	29.52	0.77	
75	356	1.1	12.5	1.07	0.016	0.71	27.94	1.0	
87.5	413	0.5	0	0	1.69	1.3	24.21	1.0	

∆ (log dw/dT)/ ∆ log wr = - E/2.303R [(∆ 1/T)/ ∆ log wr) + n

Table 20 Showing the thermal analysis results for metal complexes of ligand

Complex	Wt taken (mg)	T°C at which decomposition begins	T°C metal residue formed	Residue obtained	Wt of residue		Metal %		Water molecule	
					Found mg	Expected mg	Estimated	Calculated	Found mg	Expected mg
(FeR_2H_2O)	72.36	100	740	FeS	19.51	15.68	10.41	9.97	2.4	2.3
$CoR_2(H_2O)_2$	40.75	210	470	$CoSO_4$+ CoS	45.59	42.30	20.86	20.30	3.0	2.5
$(NiRCl)_n$	41.75	180	550	NiS	30.71	26.89	17.87	17.41	-	-
(NiR_2)	41.87	180	520	$NiSO_4$	33.11	29.06	12.56	10.80	-	-
$(CuRCl)_2$	83.71	180	795	$CuSO_4$	52.22	46.65	19.00	18.58	-	-
$(CuRClO_4)_2$	44.24	140	740	$CuSO_4$	38.96	39.29	15.52	15.65	-	-
$(CuR)_2$	29.89	220	780	$CuSO_4$	56.51	52.04	20.51	20.26	-	-
(CuR_2H_2O)	63.62	190	770	$CuSO_4$	28.95	28.10	11.53	11.19	2.4	2.01

Table 21. Showing % wt. loss at different temperatures for ligand and its metal complexes

HONNDPTu		$(CuRCl)_2$		$(CuR)_2$		(CuR_2H_2O)		$(CuRClO_4)_2$		$(NiRCl)_n$		(NiR_2)		$CoR_2(H_2O)_2$		(FeR_2H_2O)	
% wt loss	T^oC	% wt loss	T^oC	% wt loss	T^oC	% wt loss	T^oC	% wt loss	T^oC	% wt loss	T^oC	% wt loss	T^oC	% wt loss	T^oC	% wt loss	T^oC
0	293	0	353	0	313	0	363	0	363	0	313	0	293	0	353	0	313
0	433	0	453	0	493	0	373	0	413	0	453	0	453	0	413	0	353
12.5	473	11.95	573	3.3	663	3.4	423	36.1	653	40	533	52	573	7.3	433	3.3	363
25	473	23.89	703	3.3	673	3.4	463	36.1	693	40	613	52	713	7.3	483	3.3	373
37.5	483	35.01	763	43.49	1053	12.5	493	52	873	66	823	66.8	793	26.9	513	28	433
50	493	35.01	993	43.49	1173	12.5	563	52	953	66	1113	66.8	953	26.9	593	28	473
62.5	798	47.78	1068			43.7	753	61	1013					53.9	743	51	773
75	518	47.78	1173			43.7	873	61	1043					53.9	1053	51	893
87.5	573					55.9	1043									81	1013
87.5	613					55.9	1173									81	1223
100	833																
100	933																

Kinetic parameters such as the order of reaction (n), the activation energy Ea, in the decomposition process of ligand have been calculated by using Freeman and Carroll equation [50]. The different graphical representations leading to their evaluation have been drawn, Fig 36 a, b, c, d as given in Supplementary Material. The parameter values are shown in Table 19. The order of reaction for the first decomposition step is 0.35 and the activation energy is 2.3 Kcal per mole.

3.4.2 Metal complexes

The complexes of Ni(II), Fe(II), Co(II), and four complexes of different copper(II) salts, such as chloride, perchlorate, acetate, and nitrate with ligand were subjected to thermogravimetric analysis and the thermograms details are given in Table 19

From the thermograms, directly [the loss in weight due to thermal decomposition as observed at different temperatures was calculated and plotted against the respective temperatures] for each of these complexes, Table 21. The thermograms and those of [the plots of %wt loss vs T], indicate the nature of the decompositions involved, which could be classified broadly into two categories: 1) **Successive reactions –** Ligand; CuR_2H_2O; $(CuRCl)_2$;$(NiR)_2$; FeR_2H_2O and 2) **Simultaneous reactions -** $(CuR)_2$; $(CuRClO_4)_2$; $(NiRCl)_n$; $CoR_2(H_2O)_2$.

Evaluation of thermal parameters: Energy of activation Ea and order of reaction n, are calculated by difference-differential method of Freeman and Carroll from the kinetic analysis of TGA data and given below:

$$-dw/dT = Z/H\ e^{-E/RT}\ (W)^n \qquad (1)$$

and for a single thermogram, equation (1) takes the form

$$\Delta \log (dw/dT) = n\ \Delta \log Wr - (E/2.303R)\ \Delta\ 1/T) \qquad \text{……..(2)}$$

wherein - n = order of reaction; Ea = activation energy; Z = frequency factor; dw/dT = weight loss over a temperature range; H = heating rate; R – universal gas constant; W = total weight loss.

It is clear from equation (2) that when Δ 1/T is kept constant, then a plot of ΔlogdW/dT versus ΔlogWr affords a linear relationship, the slope of which yields the value of 'n' the order of reaction and the intercept value of Ea, the energy of activation. By determining the value of n and Ea, the frequency factor Z can be evaluated from equation (1).

In actual practice, for a single thermogram, another form of equation (2) as given below (3) is generally used.

$$(\Delta \log dw/dT) / (\Delta \log Wr) = -E/(2.303R) \times \Delta (1/T) / (\Delta \log Wr) \qquad (3)$$

From equation (3), a plot of left-hand side of equation (3) versus Δ 1/T / Δ log Wr provides a linear relationship whose slope will afford the value of Ea and whose intercept on X axis the value of n. Thus, the values of kinetic parameters Ea and n were evaluated for the ligand and four complexes in which the decompositions are found to follow successive reactions.

The method of evaluation of activation energy and order of reaction is given as follows:

First graph 'a' was plotted as dw versus dT, where dw is the loss in weight at any number of suitable arbitrary units of the decomposition step and dT is the T in K at that weight loss. The slope values were taken at each point thus plotted. Then the logarithm of slope values, i.e., Δ log dw/dT, was plotted against the logarithm values of Wr at each point in the graph 'b'. The slope values were evaluated for these points. The graph 'c' was obtained by plotting Δ 1/T versus Δ log Wr. This gives the slope values obtained at each point. The slope values of graph 'b' versus the slope values of graph 'c' were plotted in graph 'd' to give a linear relationship. The slope value of this graph is used to calculate the Ea and the intercept on the 'X' axis gives the order of reaction. In this way, Ea values, the order of the reaction, and the frequency factors were evaluated in the case of the ligand and the four complexes under successive types of reactions mentioned above.The respective values of dw, dT, Δ log Wr, (Δ log dw/dT) / (Δ log Wr), Δ (1/T), Δ (1/T) / Δ log Wr and the values of Ea and n are given in Tables 19 for ligand and Tables 22-25 for metal complexes, graphs were constructed for all the complexes also similar to the ones given for ligand in Fig 36 a, b, c, d.

Table 22. Showing coordinates of graphs required for Freeman and Carroll equation for $[CuRCl]_2$ complex for evaluation of kinetic parameters

wt loss dw	dT^oK	Slope values dw/dT	wr = (wc-w)	∆log wr	∆log dw/dT	Slope values ∆log dw/dT vs ∆log wr	∆ 1/T ($x10^{-4}$)	Slope values ∆ 1/T vs ∆log wr	E and n Kcal/mole
0	273	0.8	35	1.54	1.90	0.14	36.63	2	1.831
3.5	320	0.6	32	1.50	1.77	0.14	31.25	1.5	0.4
9.0	370	0.6	23	1.36	1.77	0.16	27.03	1.3	
13	420	0.75	17.5	1.24	1.87	0.5	23.87	1.0	
17.5	470	1.0	13	1.11	0.00	1.4	21.27	0.66	
23	520	1.0	9.0	0.95	0.00	6	19.23	0.66	
32	570	1.66	3.5	0.54	0.22	0.8	17.54	0.4	
35	583	1.45	0	0.00	0.16	-	17.15	-	

∆ (log dw/dT)/ ∆ log wr = - E/2.303R [(∆ 1/T)/ ∆ log wr) + n

Table 23. Showing coordinates of graphs required for Freeman and Carroll equation for $[CuR_2H_2O]$ complex for evaluation of kinetic parameters

wt loss dw	dT^oK	Slope values dw/dT	wr = (wc-w)	∆log wr	∆log dw/dT	Slope values ∆log dw/dT vs ∆log wr	∆ 1/T ($x10^{-4}$)	Slope values ∆ 1/T vs ∆log wr	E and n Kcal/mole
12.5	273	1.4	29	1.46	0.14	-	36.63	3	1.51
15	310	1.4	20	1.30	0.14	1.0	32.25	1.0	0.1
20	360	1.5	15	1.17	0.17	1.0	28.43	0.8	
29	410	2.3	12.5	1.09	0.36	1.1	24.39	0.7	
43.7	453	2.3	0	0	0.36	2	22.59	0.6	

∆ (log dw/dT)/ ∆ log wr = - E/2.303R [(∆ 1/T)/ ∆ log wr) + n

Table 24. Showing coordinates of graphs required for Freeman and Carroll equation for [NiR_2] complex for evaluation of kinetic parameters

wt loss dw	dT^oK	Slope values dw/dT	wr = (wc-w)	Δlog wr	Δlog dw/dT	Slope values Δlog dw/dT vs Δlog wr	Δ 1/T ($x10^{-4}$)	Slope values Δ 1/T vs Δlog wr	E and n Kcal/mole
0	273	1.16	52.5	1.72	0.06	0.25	36.63	5	2.3
5	295	1.16	50	1.69	0.06	0.37	33.96	1.0	0.65
27	320	1.0	42	1.62	0.00	0.12	31.25	1.0	
42	345	0.83	27	1.43	1.90	0.33	28.98	0.4	
50	370	0.43	5	0.69	1.60	0.6	27.03	0.1	
52.5	393	0.12	0	0.00	1.07	0.8	25.45	0.16	

Δ (log dw/dT)/ Δ log wr = - E/2.303R [(Δ 1/T)/ Δ log wr) + n

Table 25. Showing coordinates of graphs required for Freeman and Carroll equation for

1st decomposition step of [FeR_2H_2O] complex for evaluation of kinetic parameters									
wt loss dw	**dT^oK**	**Slope values dw/dT**	**wr = (wc-w)**	**Δlog wr**	**Δlog dw/dT**	**Slope values Δlog dw/dT vs Δlog wr**	**Δ 1/T ($x10^{-4}$)**	**Slope values Δ 1/T vs Δlog wr**	**E and n Kcal/mole**
0	273	1.5	24	1.38	0.17	1.25	36.63	-	2.75
4	285	1.8	20	1.30	0.25	0.8	35.10	0.62	0.14
8	295	2	16	1.20	0.30	0.57	33.90	0.75	
12	305	1.8	12	1.07	0.25	0.3	32.78	0.57	
16	315	1.8	8	0.9	0.25	0.14	31.75	0.43	
20	325	2	4	0.6	0.30	0.2	30.77	0.25	
24	333	1.5	0	0	0.17	-	30.03	-	
2nd decomposition step of [FeR_2H_2O] complex for evaluation of kinetic parameters									
0	273	-	52	1.71	-	-	36.63	-	4.575
29	300	0.4	50	1.69	1.60	2.6	33.26	5	0.15
31	350	0.6	45	1.65	1.77	1.0	28.57	1.66	
35	400	0.8	40	1.60	1.90	0.66	25.00	1.25	
40	450	0.8	35	1.54	1.90	0.4	22.22	1.25	
45	500	0.8	31	1.49	1.90	0.4	20.00	1.00	
50	550	1.0	29	1.46	0.00	0.33	18.18	1.00	
52	573	1.6	0	0	0.20	-	17.45	-	
3rd decomposition step of [FeR_2H_2O] complex for evaluation of kinetic parameters									
0	273	0.3	82	1.91	1.47	1.25	36.63	3.5	4.575

53	300	0.6	78	1.89	1.77	1.33	33.26	2.5	0.75
57	325	0.42	70	1.84	1.62	2.5	30.77	1.0	
63	350	1.0	63	1.79	0.00	4.5	28.57	0.75	
70	355	0.83	57	1.75	1.91	6	28.17	0.6	
78	380	0.83	53	1.72	1.91	-	26.13	0.25	
82	393	0.8	0	0	1.90	-	25.45	-	

Δ (log dw/dT)/ Δ log wr = - E/2.303R [(Δ 1/T)/ Δ log wr) + n

Table 26. Showing the stepwise decomposition of successive reactions

Compound	Step	Temperature range ^{o}C	% wt loss		Corresponding to loss of	n	E Kcal/mole
			Cald	Found			
HONNDPTu	1	160-300	72.47	73	$C_{13}H_{10}N_2O$	0.35	2.3
ligand	2	440-560	-	-	H_2S decomposing to H_2O and Sulfur to SO_2	-	-
$[CuRCl]_2$	1	180-490	37.13	38.22	C_6H_5NO	0.4	1.83
Green	2	720-795	14.88	15.68	Thioketo group	0.6	-
$[CuR_2H_2O]$	1	100-150	2.02	2.40	One water molecule	-	-
Brownish-green	2	190-290	10.9	10.8	H2O2	0.1	1.5
	3	290-480	35.5	34.38	C_6H_5 and two =NH groups	-	-
	4	600-700	20.28	21.58	Thioketo group	-	-
$[NiR_2]$	1	180-300	52.87	52.59	$(C_6H_5)_4$	0.6	5.0
Lustrous reddish brown	2	440-520	31.9	30.19	=N-C=NH &Thioketo	-	-
$[FeR_2H_2O]$	1	80-90	3.21	3.31	One water molecule	-	-
Puce or purplish-brown	2	100-160	25.28	25.73	C_6H_5-N=O and $(-NH)_2$ grps	0.1	2.75
	3	200-500	32.33	32.33	C_6H_5-N=O	0.1	4.58
	4	620-740	62.0	61.4	Thioketo C=S	0.75	4.58

Thermal behavior of individual complexes is discussed below:

Thermogram of the ligand that it decomposes in two steps. The loss in the first step in the temperature range 160-300 ^{o}C corresponds to $C_{13}H_{10}N_2O$, while the remaining component corresponding to H_2S decomposes in 400-500 ^{o}C range. The weight loss in this step corresponds to water and sulfur probably oxidises and is lost as SO_2. The energy of activation and the order of reaction of the first step have been calculated and are found to be 2.3 Kcal/mole and 0.35 Kcal/mole respectively.

In the case of four complexes decomposing simultaneously, the decomposition is found to be continuous over the temperature range 140-780 ^{o}C. Freeman and Carroll equation is not applicable for such reactions. A small deflection in each of the thermograms in the temperature range 400-700 ^{o}C corresponds to the decomposition range of thio keto group as is also found in the thermograms representing successive reactions.

The complexes $(CuRCl)_2$ and $(NiR)_2$ decompose in two steps as given in Table 26. In each case, the first step of decomposition corresponds to the loss of the organic molecules and the second step corresponds to the decomposition of the thioketo groups. Since the decomposition steps involved are of the successive type which are reported [51] to be of first order. The losses in weights, experimentally found and theoretically calculated, at each of the decomposition steps are in good agreement. The weight of the residue corresponds to $CuSO_4$, on the basis of which the molecular formula of the green Cu(II) chloride complex is represented as $(CuRCl)_2$ is confirmed. The residue corresponds to $NiSO_4$ and weight of the residue in consideration of the losses involved in the decomposition steps confirms to the molecular formula of the nickel complex (NiR_2) in conformity with the analytical data.

The complexes CuR_2H_2O and FeR_2H_2O are found to decompose in four steps, the first step corresponding to the loss of water molecules, the second and the third step corresponding to the decomposition of organic components in part while the fourth step corresponds to the decomposition of thioketo group. The parameters “Ea” and “n” the order of reaction in one of these steps have been calculated as given in Table 26. The residue corresponds to $CuSO_4$ and the weight of the residue is in conformity with the molecular formula (CuR_2H_2O). The overall value of order of the reaction is unity in conformity with the character of successive reaction. The respective energies of activation have been evaluated and shown in column VI. The residue corresponds to FeS, which confirms the molecular formula of the Fe(II) complex (FeR_2H_2O) in agreement with the analytical data.

The experimental and theoretical losses in weight at different steps of decomposition in the case of these four complexes have been calculated and tabulated in Tables 5, 8-11. In the case of complexes $(CuR)_2$, $(CuRClO_4)_2$, $NiRCl)_n$, and $CoR_2(H_2O)_2$, the decomposition is found to be continuous over the t range from 140-780 ^{o}C. Freeman and Carroll equation is not applicable to calculate any of the kinetic parameters in decompositions involving simultaneous types of reactions. However, from the nature of the thermograms it is noticed that in each of these thermograms there is a small inflection n, within the T range 600-700 deg C which corresponds to T range in which thioketo group is found to decompose in the case of thermograms representing successive reactions.

The final product of the decomposition of the complexes were found to be either a sulphide or an oxidation product of the complex, a sulphate. The residue in the case of Cu(II) and $(NiR)_2$ complexes was $CuSO_4$ and $NiSO_4$ respectively, that of $(NiRCl)_n$ and FeR_2H_2O complexes NiS and FeS respectively while the residue of $CoR_2(H_2O)_2$ complex is a mixture of $CoSO_4$ and CoS in 1:1 molar proportion.

By considering the weights of residues in each case and the weight losses involved, the molecular formula was back calculated, which was found to correspond exactly in agreement with the molecular formula arrived based on chemical analysis.

The Ni(II) complex Structure 6 satisfies the polymeric character of the complex as is inferred from the insoluble nature of the Ni(II) complex in the most common organic solvents and water.

TG study also confirms the molecular formula [NiRCl] and that the nature of the thermogram shows that the decomposition reaction of Ni(II) complex to be of simultaneous nature leading to NiS as the residue. On the basis of the above evidence, the green Ni(II) complex is a Td Ni(II)

complex and the polymeric nature may perhaps infer M-M interaction in the polymeric form and is best represented by the Structure 6 which satisfactorily explains all observed characteristic features of the complex.

4 CONCLUSION

N-(hydroxyl)-N,N-diphenyl thiourea reacts with Ni(II) chloride and Co(II) chloride to form reddish-brown complexes, puce colored Fe(II) complex and could be represented as $[MR_2]$.

Nickel forms two complexes with ligand. Green nickel (II) complex represents $[NiRCl]_n$, it is insoluble in the most common organic solvents and water, with μ = 4.4BM at RT. Based on the magnetic data, diffuse reflectance spectra, and IR spectral data, it is concluded that this is polymeric tetrahedral as in Structure 8. The other Ni(II) which is represented as $[NiR_2]$ is lustrous reddish-brown in colour and is found to be diamagnetic, and is characterized as a square-planar Ni(II) complex represented in Structure 9.Red-brown Co(II) complex is represented as $[CoR_2(H_2O)_2]$, is a high-spin complex and has a μ = 5.8 BM. The diffuse reflectance spectral band observed at 680nm is indicative of the octahedral nature of the complex, thermal data confirming presence of two water molecules, as in Structure 6. Puce colored Fe(II) complex is paramagnetic with μ = 6.3BM suggesting it to be Oh coordinated to the ligand as in Structure 4.

The solubility data indicate that the complexes formed from Cu(II) chloride, Cu(II) perchlorate, Cu(II) acetate, and Ni(II) chloride are very sparingly soluble in the most common organic solvents and water, indicating the polymeric nature of the complexes. The complexes formed from Cu(II) nitrate, Ni(II) chloride, Co(II) chloride are fairly soluble in chloroform, while the complex formed from Fe(II) sulfate decomposes in hydroxyl solvents and water.

Cu(II) salts are formed around pH 7.5, are green, light-green, and brownish-green formulated as [MRX] and $[MR_2H_2O]$ where M is Cu(II), R is the ligand with a loss of a proton, while X may be chloride or perchlorate. The brownish-green complex formed from $Cu(NO_3)_2$ is characterized as a distorted octahedral complex, the dark brown complex formed with copper (II) acetate is dimeric square-planar with nitrogen coordination.

Green, dark-brown and light green complexes formed with Cu(II) exhibited sub-normal magnetic moments, a characteristic property exhibited by dimeric copper(II) complexes with sulfur bridging between copper atoms. Abnormally low value of the magnetic moment compared to that expected for one unpaired electron is probably due to Cu-Cu interaction in the solid complex indicating the polymeric nature of these complexes. They were found to agree with Bleaney-Bower's equation at room temperature and the magnetic moment values experimentally determined well fit with the theoretical values calculated. These could be represented as square-planar complexes with trans structures, Structure 24. Brownish-green complex has μ = 1.9BM, indicating it to be probably an Oh or distorted Oh structure for the Cu(II) complex, Structure 25.

All complexes and the ligand were subjected to thermal degradation. The decomposition curves were obtained as dynamic curves with a linear increase of temperature with a heating rate of 6 ^oC /min. The % weight loss is calculated at each step and it is observed that in all complexes thioketo group is lost at very high temperatures. Metal estimations were back calculated and the residues established confirmed with the analytical data and gravimetric metal estimations. They were all broadly classified into two categories, four of successive and four of simultaneous type of reactions. Thermal decomposition properties are discussed in detail in the light of Freeman and Carroll equations. This difference-differential method was utilized for evaluating the kinetic parameters like order of reaction and energy of activation, obtained from the plots of linear graphs drawn at various stages of decomposition in successive reactions, all results are discussed and tabulated.

DEDICATION OF THIS ARTICLE

- Dedicated to my mom, guide, mentor - (Late) Dr T Mangamamba, Reader in chemistry, Osmania University, Hyderabad, India, for her 75th birthday.

ACKNOWLEDGEMENTS

The author would like to thank all the concerned people at various institutions who helped her to use the equipment required for the research work. Especially the help and support from Mr G Radhakrishna and Dr Mukesh Shrivatsava are greatly appreciated.

COMPETING INTERESTS

Authors have declared that no competing interests exist.

REFERENCES

1. Shadab Mohd, Aslam M. Synthesis and Characterization of Some Transition Metal complexes with N-phenyl-N'-[substituted phenyl] Thiourea. Mat Sci Res India. 2014;11(1):83-9. Available:https://doi.org/10.13005/msri/110111
2. K.MW. Chem Sci J. 2020;11. Available:https://doi.org/10.37421/csj.2020.11.208
3. Chayah M, Camacho ME, Carrión MD, Gallo MA, Romero M, Duarte J. N , N ′-Disubstituted thiourea and urea derivatives: design, synthesis, docking studies and biological evaluation against nitric oxide synthase. MedChemComm. 2016;7(4):667-78. Available:https://doi.org/10.1039/c5md00477b
4. Ozturk II, Yarar S, Banti CN, Kourkoumelis N, Chrysouli MP, Manoli M et al.. QSAR studies on antimony(III) halide complexes with N-substituted thiourea derivatives. Polyhedron. 2017;123:152-61. Available:https://doi.org/10.1016/j.poly.2016.11.008
5. Journal I, Hassan AM, Elbialy ZI, Wahdan KM. Organic & medicinal chem IJ9; 2020. Available:https://doi.org/10.19080/OMCIJ.2020.09.555767
6. Ajibade PA, Zulu NH Zulu. Metal complexes of diisopropylthiourea: synthesis, characterization and antibacterial studies. Int J Mol Sci. 2011;12(10):7186-98. Available: https://doi.org/10.3390/ijms12107186
7. Rakhshani S, Rezvani AR, Dušek M, Eigner V. Design and fabrication of novel thiourea coordination compounds as potent inhibitors of bacterial growth. J Antibiot (Tokyo). 2019;72(5):260-70. doi: 10.1038/s41429-019-0147-2, PMID 30755737.
8. Mansour AM, Shehab OR. Spectroscopic and TDDFT studies of N-phenyl-N′-(3-triazolyl)thiourea) compounds with transition metal ions. Arab J Chem. 2021;14(2). Available: https://doi.org/10.1038/s41429-019-0147-2
9. Mathur N, Jain N, Sharma AK. Synthesis, Characterization and Biological Analysis of Some Novel Complexes of Phenyl Thiourea Derivatives with Copper. CHEM. 2019;5(1):182-95. Available:https://doi.org/10.2174/1874842201805010182
10. Al-Riyahee AAA, Horton PN, Coles SJ, Berry C, Horrocks PD, Pope SJA et al., BASRA JOURNAL OF SCIENCE39 (2021) 96–118. N,N'-Substituted thioureas and their metal complexes: syntheses, structures and electronic properties. Dalton Trans. 2022;51(9):3531-45. Available:https://doi.org/10.29072/basjs.202117
11. Swarnabala G [MSc thesis] submitted to The University of Bombay; December 6, 1982, Structural Investigation of Metal Complexes, of N(hydroxyl)-N,N-diphenyl Thiourea, and references therein.
12. Mishra A, Sharma P, Soni N, Awate R. Synthesis and characterization of metal complexes of 3-(N -phenyl)-thiourea-pentanone-2. J Coord Chem. 2008;61(22):3687-92. Available:https://doi.org/10.1080/00958970802123477
13. Dwarakanath K, Sathyanarayana DN, Current Science Association. 1978;47:706-8. Available:https://www.jstor.org/stable/24082155.
14. Rathakrishnan S, Jameel A, Syed A, Padusha M. Int J Sci Res Publi. 2014;4:1-8. Available: http://www.ijsrp.org/e-journal.html
15. Holt SL, Carlin RL, Chem M. LaB12. [doctoral thesis] submitted to Brown University, June 1965. p. 3017-24 and references therein; 1964. Available: https://datapdf.com/some-transition-metal-complexes-of-substituted-thioureas-11-.html
16. Arora OP, Sankhla DS, Mishra SN. Proc Indian Natl Sci Acad. 1980;46A(4):378-80.
17. Askalani P, Bailey RA. Can J Chem. 1969;47:2275-82. Available: chrome-extension://efaidnbmnnnibpcajpcglclefindmkaj.
18. Morgan GT, Burstall FH. XXI.—researches on residual affinity and co-ordination. Part XXX. Complex ethylenethiocarbamido-

salts of univalent and bivalent metals. J Chem Soc. 1928;143:143-55.
Available:https://doi.org/10.1039/JR9280000143

19. Larkworthy LF, Nelson-Richardson MHO. Complexes of chromium(II) halides with thiourea and substituted thioureas. Inorganica Chimica Acta. 1980;40:217-21.
Available: https://doi.org/10.1016/S0020-1693(00)92008-5
20. Swarnabala G, Khatavkarand SB, Sadana GS, All India Science Congress, Tirupati. Structural investigations of metal complexes of N-(hydroxy)-N,N-diphenyl thiourea; January 1983.
21. Swarnabala G, Khatavkarand SB, Sadana GS. Thermal studies of some transition metal complexes of N-(hydroxy)-N,N-diphenyl thiourea, Annual Convention of Chemists held at Cuttack; December 26-30; 1983.
22. Guoy LG, ComptesRendus. 1889;935.
Available:https://www.biodiversitylibrary.org/item/23727#page/1043/mode/1up
23. Figgis BB. Modern coordination chemistry Lewis J, Wilkins RG, editors. New York: Interscience; 1960.
24. Dains FB, Brewster RQ, Olander CP. Organic synthesis. 1926;1:6 72.
Available:http://www.orgsyn.org/demo.aspx?prep=CV1P0447.
25. Jeffery GH, Bonnett J, Mendham J, Denney RC. A Text book of Quantitative Inorganic analysis. Vol. 497(479), 309. New York: Wiley and sons, 1975;3:529-628.
26. Hasan M, Mathur SP, Mehta VP, Bhandari CS. Indian J Technol. 1978;16:123.
27. Soni PL. Text book of Organic Chemistry, Sultanchand and sons, New Deihi. 1980;1:35-42.
28. Yoe JH, Jones AL. Ind. Eng. Chem. 1944;111-115:Anal16.
Available:
https://doi.org/10.1021/i560126a015
29. Vosburgh WC, Cooper GR. Complex Ions. I. The Identification of Complex Ions in Solution by Spectrophotometric Measurements. J Am Chem Soc. 1941;63(2):437-42.
Available:https://doi.org/10.1021/ja01847a025
30. Job P. Ann Chim. 1928;9:113-203[CAS]. Google Scholar.
31. Gupta SL, Soni RN, Jaitly JN. [CAS]. J Indian Chem Soc. 1966;43:331. Google Scholar.
32. Bleaney B, Bowers KD. Proc R Soc Lond A. 1952;214:451,
Available: chrome-extension://efaidnbmnnnibpcajpcglclefindmkaj.
33. Dwarakanath K, Satyanarayana DN. Indi. J Chem. 1979;24:302.
34. Khatavkar SB, Haldar BC. Structural investigations of nickel(II) complexes of isonitrosoacetylacetone. J Inorg Nucl Chem. 1974;36(10):2239-45.
Available: https://doi.org/10.1016/0022-1902(74)80261-7
35. Suzuki I. Infrared Spectra and Normal Vibrations of Thioamides. III. N - Methylthioformamide and N - Methylthioacetamide. Boll Chem Soc. 1962;35(9):1456-64. Available: https://doi.org/10.1246/bcsj.35.1456
36. Rao CNR, Chaturvedi GC. Normal vibrations of N-methylthioacetamide. Spectrochim Acta A Mol Spectrosc A. 1971;27(3):520-2.
Available:http://old.jncasr.ac.in/cnrrao/1971.html
37. Geetharani K, Satyanarayana DN. Indian J Chem A. 1976;14(03):170-3.
Available:
http://nopr.niscpr.res.in/handle/123456789/53638
38. Maki G. Ligand Field Theory of Ni(II) Complexes. III. Electronic Spectra and Solution Paramagnetism of Some Diamagnetic Ni(II) Complexes. J Chem Phys. 1958;29(5):1129-38.
Available: chrome-extension://efaidnbmnnnibpcajpcglclefindmkaj/
https://etd.ohiolink.edu/apexprod/rws_etd/send_file/send?accession=osu1486562013353342&disposition=inline
39. Manch W, Fernelius WC. J Chem Educ. 1963;40:260. Manch W, Fernelius WC. The structure and spectra of nickel(II) and copper(II) complexes. J Chem Educ. 1961;38(4):192.
Available: chrome-extension://efaidnbmnnnibpcajpcglclefindmkaj. doi: 10.1021/ed038p192.
40. Mecke RMR, Luthingham R. Chem Ber. 1957;90:975-86.
Available:https://doi.org/10.1002/cber.19570901117
41. Gosavi RK, Agarwala U, Rao CNR. Infrared Spectra and Configuration of Alkylthiourea Derivatives. Normal Vibrations of N,N′-Dimethyl- and

Tetramethylthiourea. J Am Chem Soc. 1967;89(2):235-9.
Available:https://doi.org/10.1021/ja00978a009

42. Gosavi RK, Rao CNR. Infrared absorption spectra of metal complexes of alkylthioureas and some related ligands. J Inorg Nucl Chem. 1967;29(8):1937-45.
Available: https://doi.org/10.1016/0022-1902(67)80453-6
43. Tucker I, Singh RP, Zacharias PS. [CAS]. Indian J Chem. 1979;18A:60. Google Scholar.
44. Cotton FA, Wilkinson G. Wiley eastern Ltd. Adv Inorg Chem. 1980.
45. Klemn W, Schuth W, Anorg Z, Allgem. [Crossref]. Chem. 1931;203:104. Google Scholar.
46. Muto Y. Metal Complexes with Terdentate Ligands. II. Synthesis and Properties of Tri-coordinated Copper(II) Complexes. Bull Chem Soc Jpn. 1960;33(9):1242-7.
Available:https://doi.org/10.1039/JR9610000312.
47. Walls AF. Structural Inorganic chemistry. 1962;463:591, 873.
48. Nickless G. Amsterdam, London: Inorganic Sulfur Chemistry, Elsevier Publishing company; 1968.
49. Chhatwal. Anand, Instrumental methods of Analysis. 1st ed. Himalayan Publishing House; 1979.
50. Freeman ES, Carroll B. The Application of Thermoanalytical Techniques to Reaction Kinetics: The Thermogravi-metric Evaluation of the Kinetics of the Decomposition of Calcium Oxalate Monohydrate. J Phys Chem. 1958;62(4):394-7.
Available:http://dx.doi.org/10.1021/j150562a003
51. Reiche L, Stivala SS. Elements of polymer degradation. Gracan Hill Limited; 1979.

APPENDIX

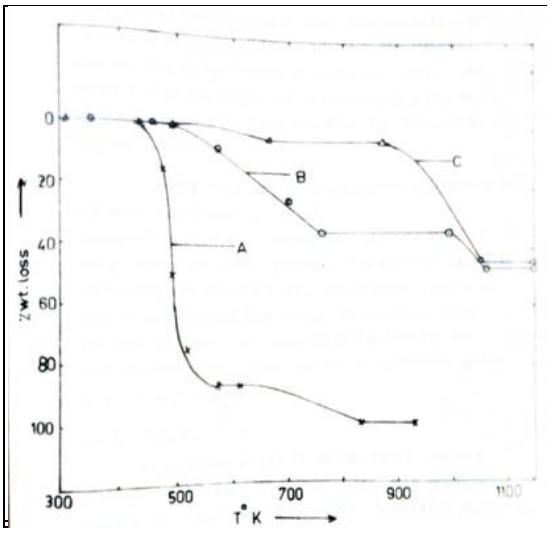

Fig. 33. Thermogram of %wt loss vs temp K for A reagent, B $(CuRCl)_2$, C $(CuR)_2$

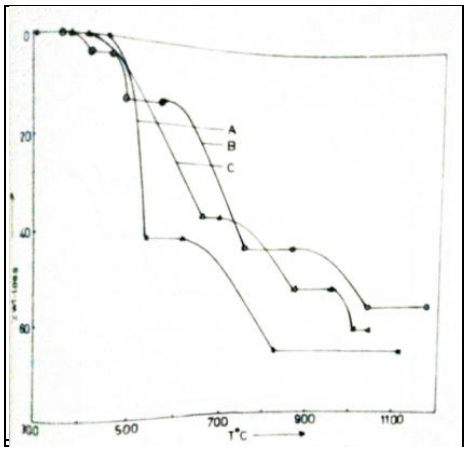

Fig. 34. Thermogram of %wt loss vs temp K for A $(NiRCl)_n$, B CuR_2H_2O, C $(CuRClO_4)_2$

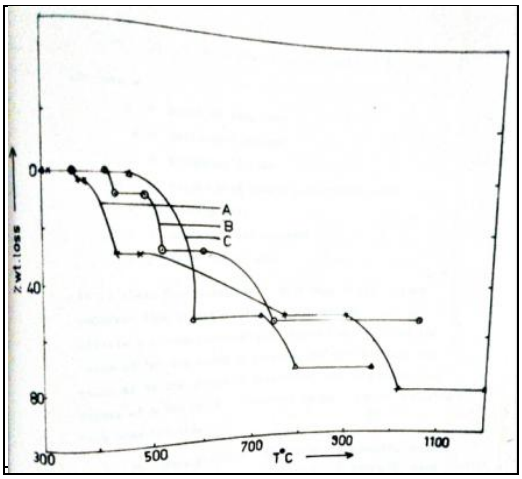

Fig. 35. Thermogram of %wt loss vs temp K for A FeR_2H_2O, B $CoR_2(H_2O)_2$, C NiR_2

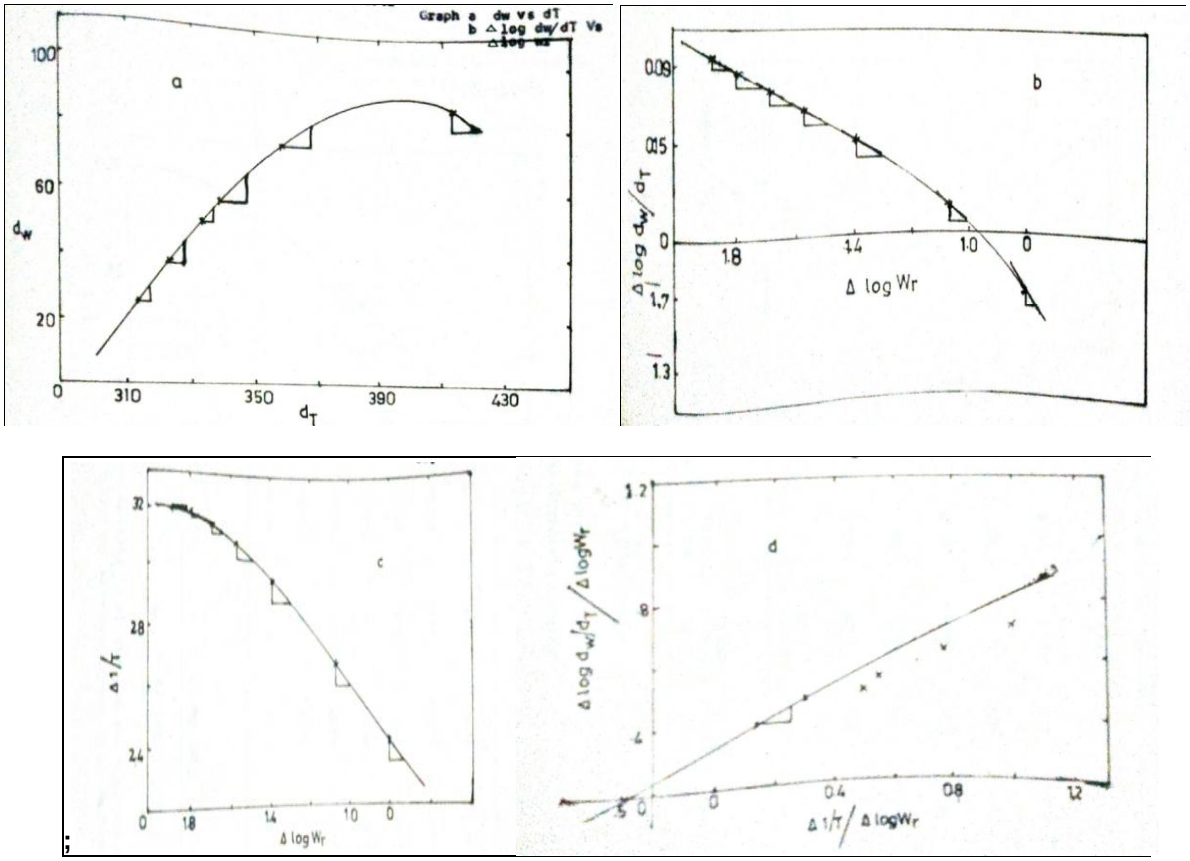

Fig. 36. a, b, c, d. Graphs showing the details of parametric calculations as required by Freeman and Carroll equation for HONNNDPTu

Graph a – dw vs dT; b – ∆ log dw/dT vs ∆ log wr; c – ∆ (1/T) vs ∆ log Wr; d- (∆log dw/dT vs ∆log wr) vs ∆ (1/T) vs ∆ log Wr

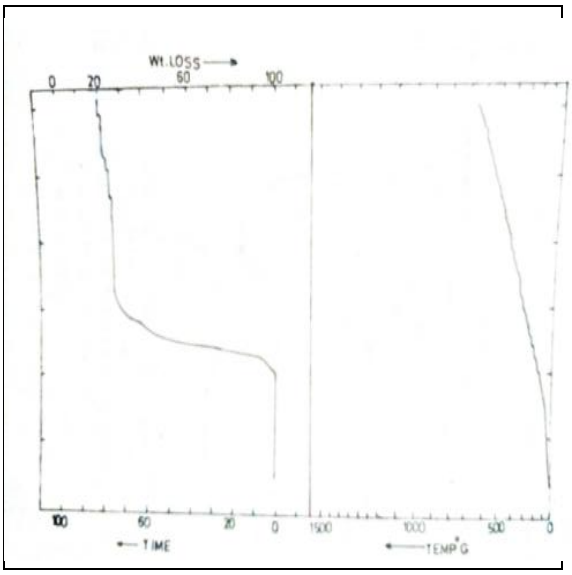

Fig. 31. Thermogram obtained from instrument for Reagent

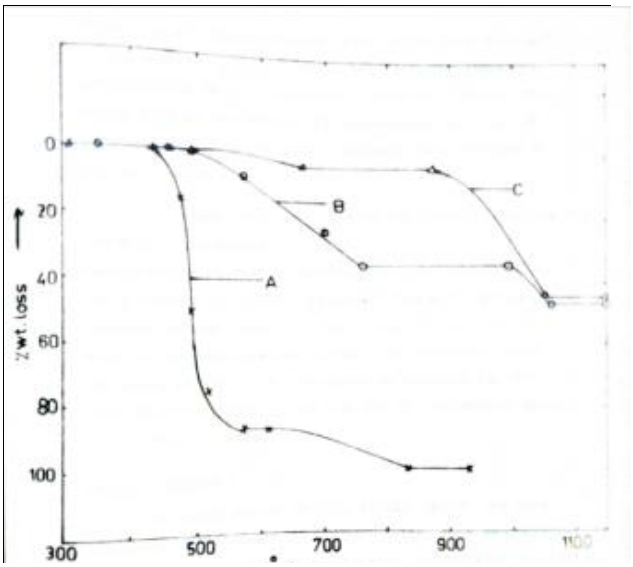

Fig. 32. Thermogram of %wt loss vs temp K, for A=Reagent, B=$(CuRCl)_2$, C=$(CuR)_2$

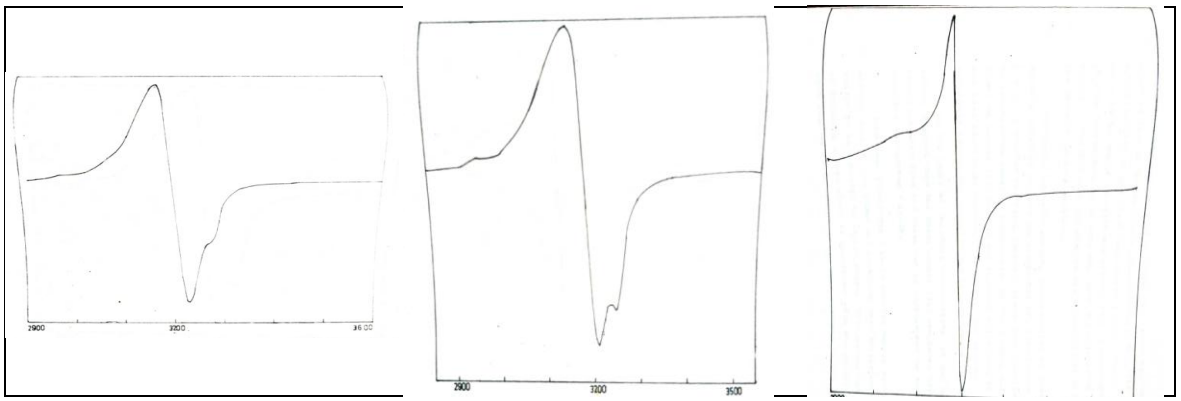

Figs. 14-16. ESR spectra obtained from instrument for $(CuRCl)_2$, $(CuRClO_4)_2$ and $(CuR)_2$

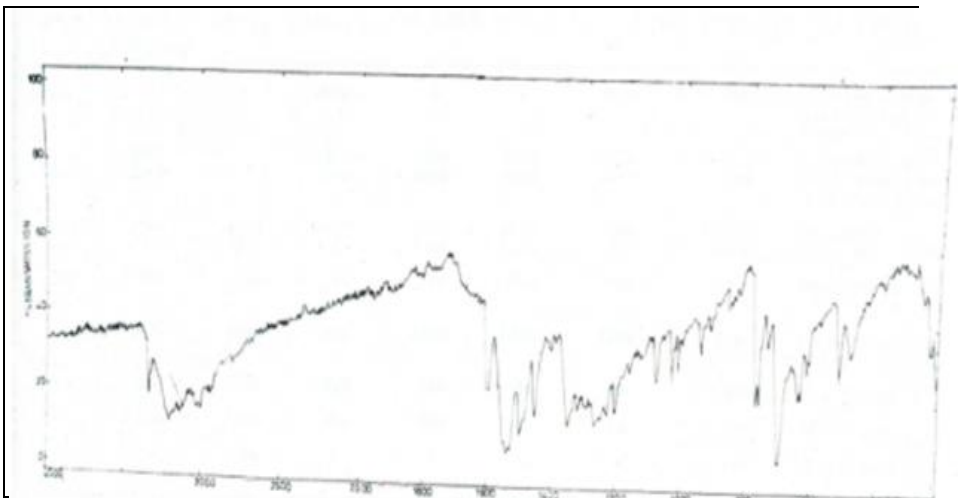

Fig. 2. IR spectrum of Ligand

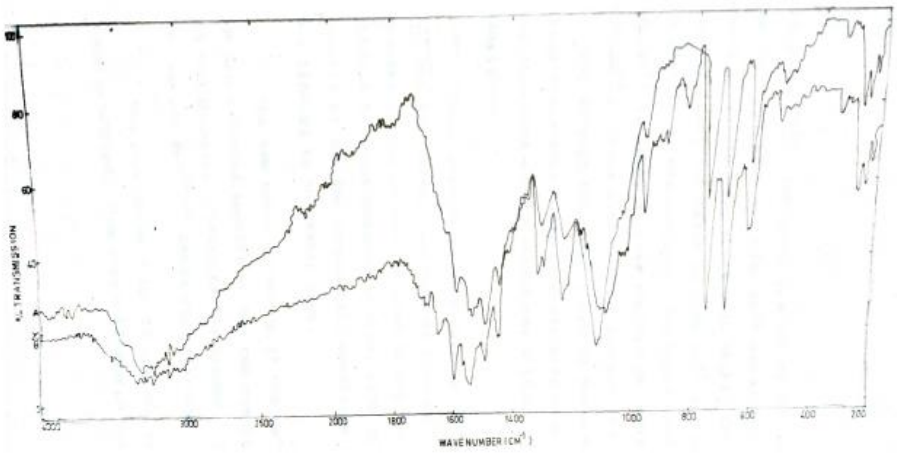

Fig. 3. IR spectrum of FeR_2H_2O complex

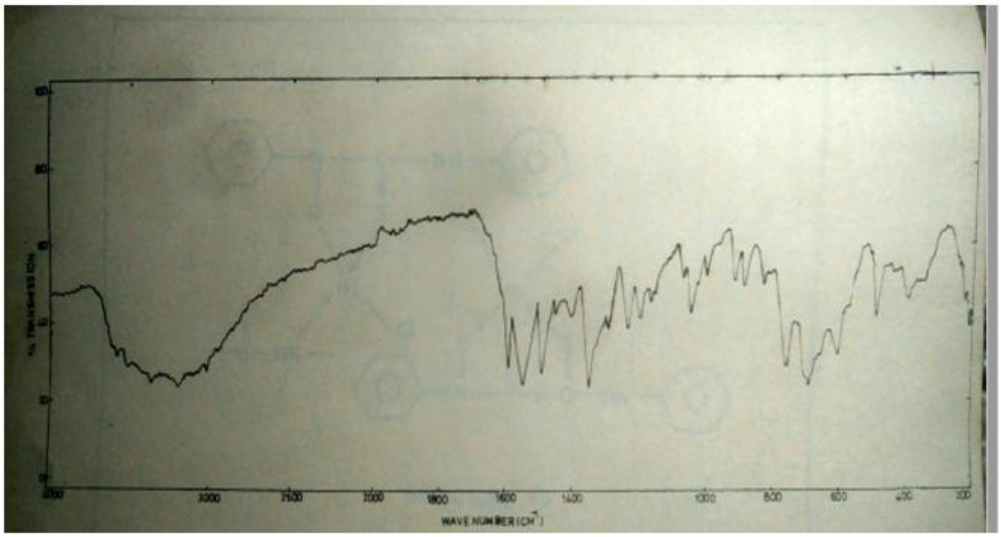

Fig. 4. IR spectrum of $(NiR_2Cl)n$ complex

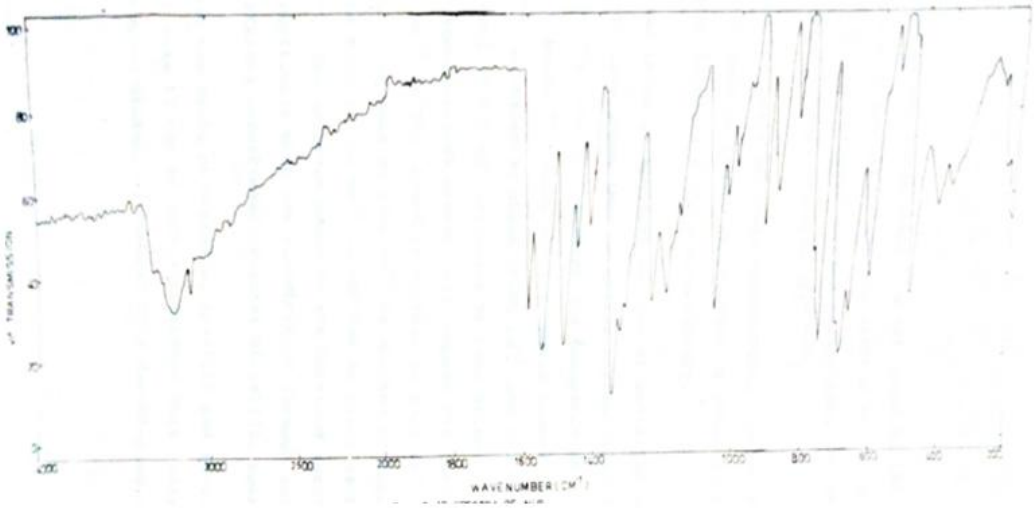

Fig. 5. IR spectrum of NiR_2 complex

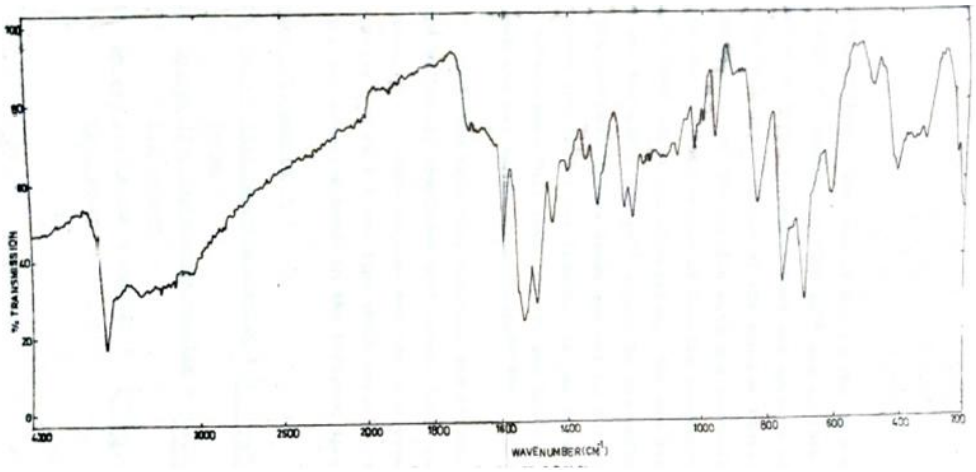

Fig. 6. IR spectrum of $CoR_2(H_2O)_2$ complex

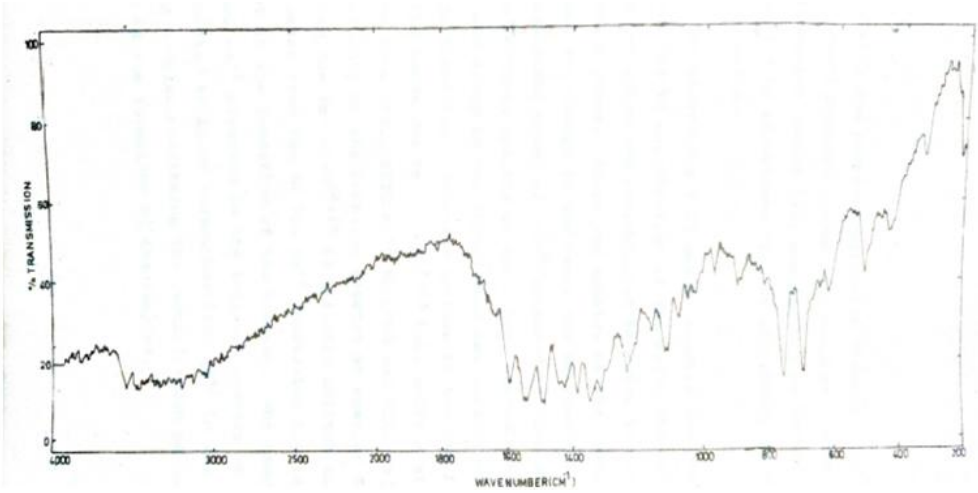

Fig. 7. IR spectrum of CuR_2H_2O complex

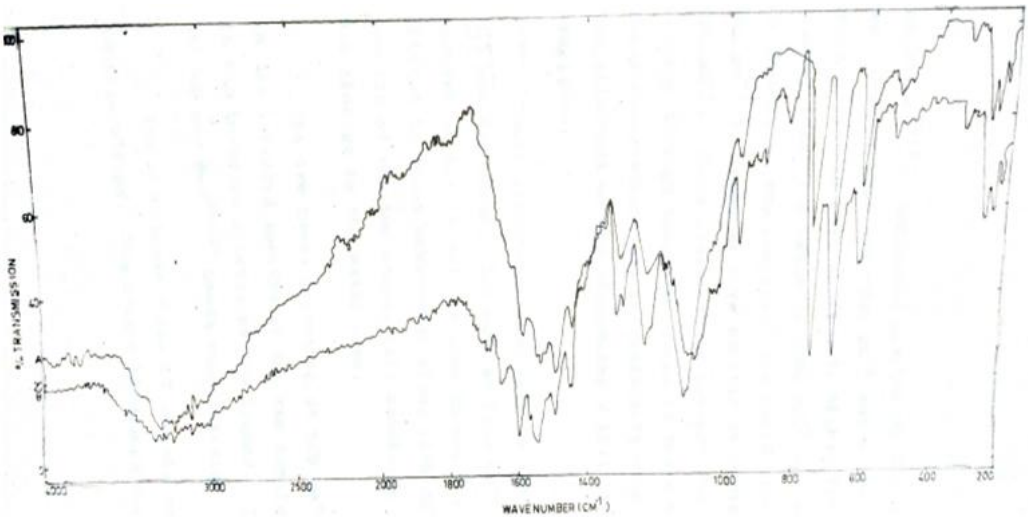

Fig. 8 & 9. IR spectrum of A-$(CuRCl)_2$ and B-$(CuRClO_4)_2$ complex

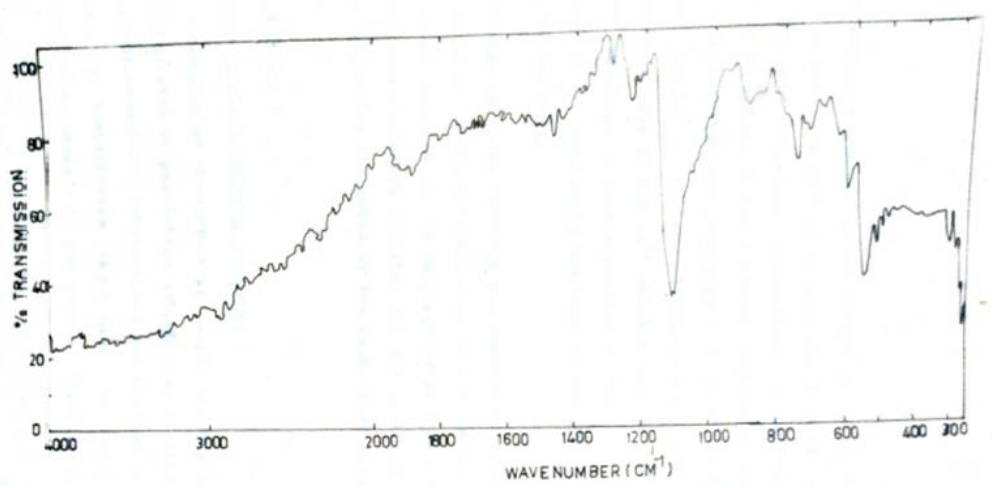

Fig. 10. IR spectrum of $(CuR)_2$ complex

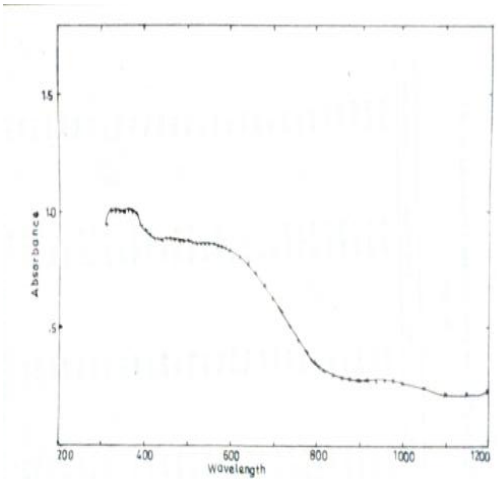

Wavelength	Absorbance	Wavelength	Absorbance
1200	0.234	560	0.860
1150	0.220	550	0.865
1100	0.210	540	0.867
1050	0.242	530	0.865
1000	0.264	520	0.870
980	0.275	510	0.870
960	0.270	500	0.875
940	0.270	490	0.875
920	0.275	480	0.872
900	0.279	470	0.880
880	0.280	460	0.885
860	0.282	450	0.885
840	0.294	440	0.880
820	0.314	430	0.885
800	0.350	420	0.897
780	0.395	410	0.902
760	0.445	400	0.920
740	0.508	390	0.945
720	0.570	380	0.990
700	0.625	370	1.010
680	0.680	360	1.030
660	0.733	350	1.040
640	0.773	340	1.040
620	0.804	330	1.030
600	0.835	320	1.020
590	0.845	310	0.945
580	0.850	300	1.900
	0.855		

Fig. 11. Diffuse Reflectance Spectra of FeR_2H_2O complex drawn using data in Table 4

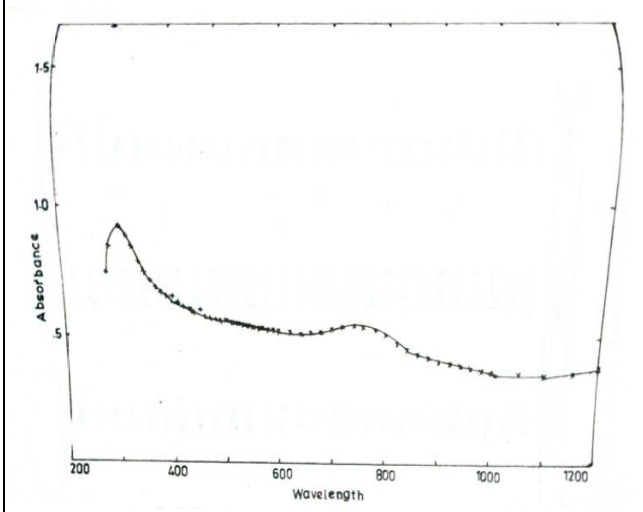

Wavelength	Absorbance	Wavelength	Absorbance
1200	0.370	570	0.530
1150	0.355	560	0.530
1100	0.347	550	0.537
1050	0.355	540	0.540
1000	0.361	530	0.545
980	0.365	520	0.550
960	0.372	510	0.553
940	0.382	500	0.562
920	0.390	490	0.560
900	0.397	480	0.570
880	0.410	470	0.570
860	0.427	460	0.580
840	0.445	450	0.605
820	0.465	440	0.595
800	0.485	430	0.610
780	0.500	420	0.620
760	0.507	410	0.637
740	0.515	400	0.660
720	0.530	390	0.665
700	0.520	380	0.675
680	0.512	370	0.695
660	0.512	360	0.725
640	0.508	350	0.765
620	0.512	340	0.800
600	0.520	330	0.852
590	0.525	320	0.895
580	0.527	310	0.930

Fig.12. Diffuse Reflectance Spectra of (NiRCl)n drawn using the data given in Table 5

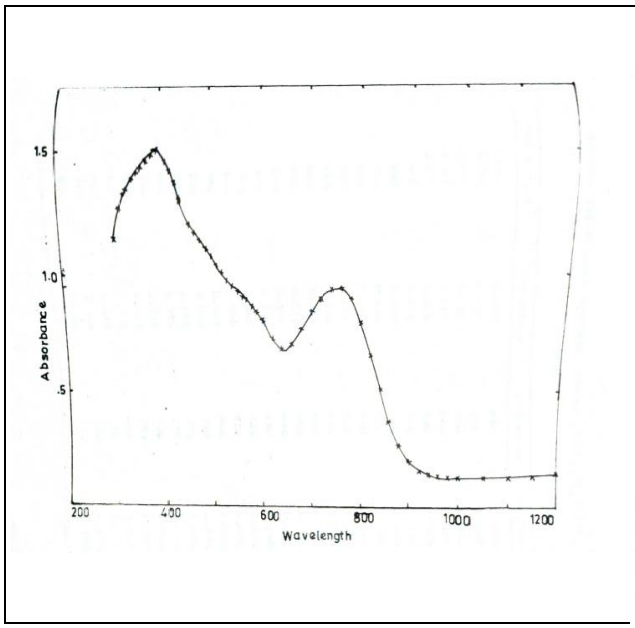

Wavelength	Absorbance	Wavelength	Absorbance
1200	0.150	570	0.900
1150	0.138	560	0.915
1100	0.125	550	0.940
1050	0.127	540	0.960
1000	0.128	530	0.985
980	0.125	520	1.020
960	0.130	510	1.040
940	0.136	500	1.090
920	0.153	490	1.110
900	0.191	480	1.150
880	0.266	470	1.180
860	0.365	460	1.220
840	0.510	450	1.320
820	0.660	440	1.310
800	0.800	430	1.380
780	0.900	420	1.420
760	0.945	410	1.460
740	0.945	400	1.500
720	0.900	390	1.470
700	0.850	380	1.430
680	0.773	370	1.430
660	0.707	360	1.400
640	0.687	350	1.390
620	0.735	340	1.330
600	0.815	330	1.320
590	0.850	320	1.270
580	0.875	310	1.150

Fig. 13. Diffuse Reflectance Spectra of $(NiR)_2$ drawn using the data given in Table 6

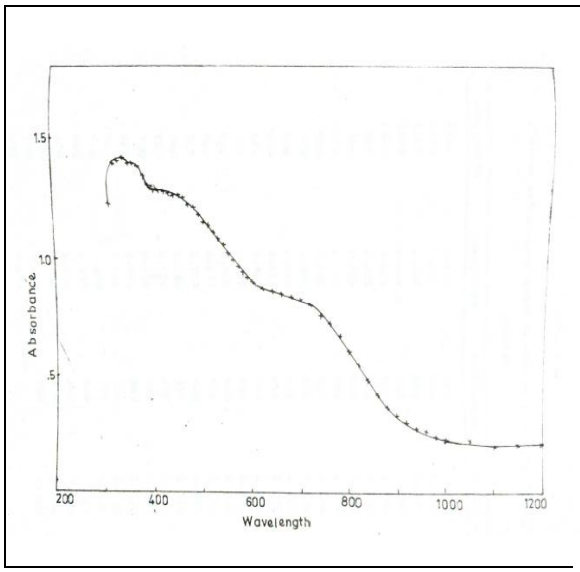

Wavelength	Absorbance	Wavelength	Absorbance
1200	0.202	560	1.000
1150	0.206	550	1.030
1100	0.192	540	1.070
1050	0.218	530	1.090
1000	0.222	520	1.120
980	0.235	510	1.150
960	0.258	500	1.160
940	0.270	490	1.190
920	0.296	480	1.220
900	0.325	470	1.230
880	0.360	460	1.260
860	0.415	450	1.270
840	0.480	440	1.270
820	0.545	430	1.280
800	0.605	420	1.290
780	0.677	410	1.290
760	0.727	400	1.290
740	0.760	390	1.310
720	0.810	380	1.350
700	0.825	370	1.390
680	0.840	360	1.400
660	0.855	350	1.400
640	0.865	340	1.420
620	0.875	330	1.410
600	0.905	320	1.400
590	0.925	310	1.230
580	0.950	300	1.900
570	0.975		

Fig. 14. Diffuse Reflectance Spectra of $CoR_2(H_2O)_2$ drawn using the data given in Table 7

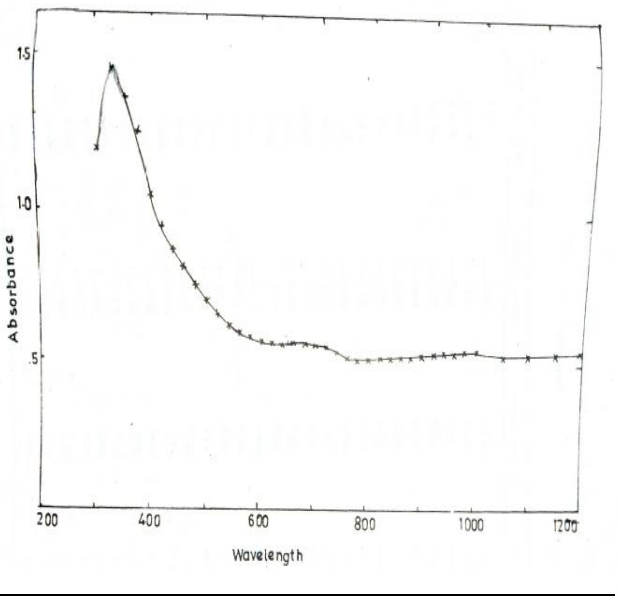

Wavelength	Absorbance	Wavelength	Absorbance
1200	0.555	570	0.590
1150	0.545	560	0.600
1100	0.532	550	0.615
1050	0.525	540	0.625
1000	0.545	530	0.635
980	0.540	520	0.660
960	0.525	510	0.680
940	0.535	500	0.710
920	0.530	490	0.720
900	0.520	480	0.760
880	0.520	470	0.780
860	0.520	460	0.818
840	0.505	450	0.845
820	0.505	440	0.880
800	0.510	430	0.915
780	0.510	420	0.950
760	0.515	410	0.990
740	0.520	400	1.040
720	0.520	390	1.100
700	0.530	380	1.210
680	0.535	370	1.290
660	0.540	360	1.370
640	0.540	350	1.430
620	0.550	340	1.470
600	0.565	330	1.480
590	0.575	320	1.380
580	0.585	310	1.190

Fig . 15. Diffuse Reflectance Spectra of CuR_2H_2O drawn using the data given in Table 8

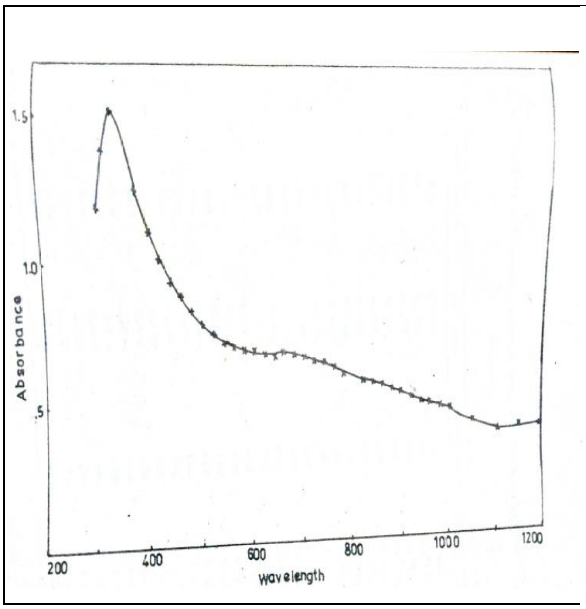

Wavelength	Absorbance	Wavelength	Absorbance
1200	0.395	570	0.695
1150	0.390	560	0.710
1100	0.387	550	0.717
1050	0.410	540	0.725
1000	0.455	530	0.730
980	0.465	520	0.750
960	0.462	510	0.775
940	0.495	500	0.790
920	0.510	490	0.815
900	0.520	480	0.840
880	0.540	470	0.860
860	0.540	460	0.895
840	0.555	450	0.920
820	0.570	440	0.945
800	0.585	430	0.985
780	0.600	420	1.020
760	0.620	410	1.050
740	0.637	400	1.110
720	0.648	390	1.160
700	0.660	380	1.260
680	0.668	370	1.340
660	0.676	360	1.400
640	0.670	350	1.470
620	0.675	340	1.520
600	0.690	330	1.540
590	0.695	320	1.410
580	0.695	310	1.190

Fig. 16. Diffuse Reflectance Spectra of $(CuRClO_4)_2$ drawn using the data given in Table 9

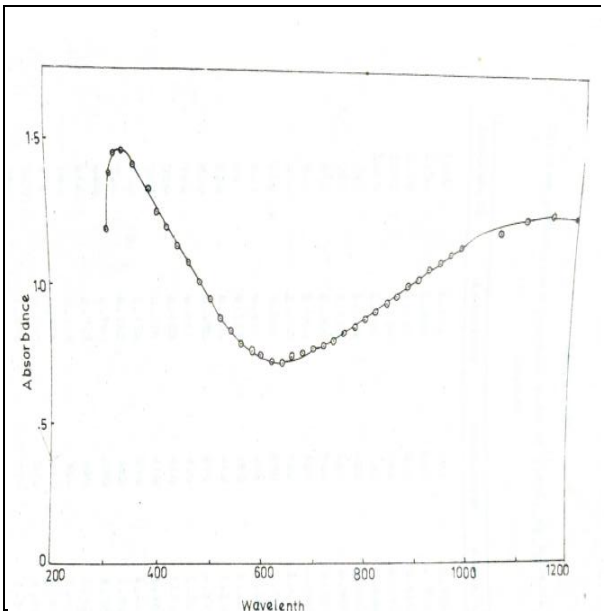

Wavelength	Absorbance	Wavelength	Absorbance
1200	1.240	570	0.775
1150	1.250	560	0.793
1100	1.230	550	0.810
1050	1.190	540	0.830
1000	1.200	530	0.860
980	1.140	520	0.880
960	1.110	510	0.905
940	1.080	500	0.950
920	1.060	490	0.965
900	1.020	480	1.010
880	1.000	470	1.030
860	0.960	460	1.080
840	0.935	450	1.100
820	0.905	440	1.130
800	0.875	430	1.170
780	0.845	420	1.200
760	0.825	410	1.220
740	0.795	400	1.250
720	0.775	390	1.280
700	0.765	380	1.250
680	0.750	370	1.380
660	0.737	360	1.410
640	0.718	350	1.450
620	0.725	340	1.450
600	0.745	330	1.450
590	0.755	320	1.380
580	0.760	310	1.190

Fig. 17. Diffuse Reflectance Spectra of $(CuRCl)_2$ drawn using the data given in Table 10

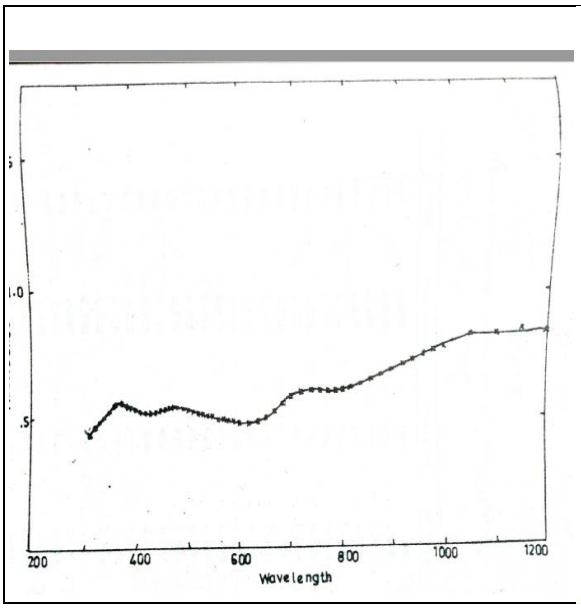

Wavelength	Absorbance	Wavelength	Absorbance
1200	0.840	560	0.495
1150	0.852	550	0.505
1100	0.830	540	0.507
1050	0.835	530	0.515
1000	0.783	520	0.520
980	0.770	510	0.528
960	0.750	500	0.535
940	0.732	490	0.540
920	0.715	480	0.540
900	0.690	470	0.545
880	0.670	460	0.546
860	0.653	450	0.560
840	0.632	440	0.545
820	0.615	430	0.550
800	0.595	420	0.545
780	0.575	410	0.545
760	0.600	400	0.545
740	0.543	390	0.537
720	0.525	380	0.530
700	0.515	370	0.530
680	0.502	360	0.525
660	0.495	350	0.515
640	0.485	340	0.497
620	0.480	330	0.485
600	0.484	320	0.475
590	0.490	310	0.462
580	0.490	300	0.510
570	0.495		

Fig. 18. Diffuse Reflectance Spectra of $(CuR)_2$ drawn using the data given in Table 11

Peer-review history:
The peer review history for this paper can be accessed here:
https://www.sdiarticle5.com/review-history/92374